# RSC Sustainability

## Accepted Manuscript

**RSC Sustainability**

ROYAL SOCIETY OF CHEMISTRY

This is an Accepted Manuscript, which has been through the Royal Society of Chemistry peer review process and has been accepted for publication.

Accepted Manuscripts are published online shortly after acceptance, before technical editing, formatting and proof reading. Using this free service, authors can make their results available to the community, in citable form, before we publish the edited article. We will replace this Accepted Manuscript with the edited and formatted Advance Article as soon as it is available.

You can find more information about Accepted Manuscripts in the Information for Authors.

Please note that technical editing may introduce minor changes to the text and/or graphics, which may alter content. The journal's standard Terms & Conditions and the Ethical guidelines still apply. In no event shall the Royal Society of Chemistry be held responsible for any errors or omissions in this Accepted Manuscript or any consequences arising from the use of any information it contains.

ROYAL SOCIETY OF CHEMISTRY

## Sustainability Spotlight Statement

Wearable electronic devices necessitate high-energy flexible energy storage devices. Flexible batteries with carbon-based fibrous electrodes attracted the modern gadgetries due to their high bendability and twistability. Development of sustainable batteries are utmost important to achieve the UN Sustainable Development Goal: 7: Affordable and Clean Energy. Carbon-based flexible electrodes are highly sustainable materials to develop flexible batteries for next-generation wearable electronic devices.

# Recent Progresses in the Synthesis and Strategic Designs of Sustainable Carbon-Based Fibrous Electrodes for Flexible Batteries

Susmi Anna Thomas[1], Jayesh Cherusseri[2,3]* and Deepthi N. Rajendran[1]*

[1]Department of Physics, Government College for Women (Affiliated to University of Kerala), Thiruvananthapuram, Kerala 695014, India
[2]Research Centre for Nanomaterials and Energy Technology (RCNMET), School of Engineering and Technology, Sunway University, No. 5, Jalan Universiti, Bandar Sunway, 47500 Selangor Darul Ehsan, Malaysia
[3]School of Engineering and Technology, Sunway University, No. 5, Jalan Universiti, Bandar Sunway, 47500 Selangor Darul Ehsan, Malaysia

**\*Corresponding Author**
E-Mail Address: drjayeshpuli@gmail.com (JC); deepthinrphysics@gmail.com (DNR)

## Abstract
Electrochemical energy storage devices such as rechargeable batteries and supercapacitors have replaced conventional batteries and dielectric capacitors due to their excellent charge storage abilities and other electrochemical performances. But the major challenge exists in terms of their flexibility in application as most of the rechargeable batteries and supercapacitors available commercially are rigid in nature hence cannot be used in wearable electronic applications. The flexibility to the devices is mainly imparted by the electrodes hence the preparation of electrodes is utmost important in determining their flexibility. During the fabrication of electrodes, the electrode-active materials are coated over an electrically conducting substratum and it is further used as a current collector for the electrode. The electrodes will be flexible if the substratum used for the preparation is flexible in nature. In this aspect, carbon fiber (CF) evolved as suitable and sustainable substratum for the preparation of electrodes for rechargeable batteries to power flexible electronic devices. Micron-sized or nano-sized CF are invariably used as substratum hence the flexibility can easily be imparted to the devices assembled. This review outlines the development of rechargeable batteries manufactured of different electrode-active materials coated over this CF substratum. This article helps to get an in-depth insight about the preparation of flexible electrodes for rechargeable batteries, particularly for application in wearable electronics.

**Keywords:** Rechargeable batteries, lithium-ion batteries, sodium-ion batteries, Carbon fibers, Wearable electronics, Sustainable energy.

## 1. Introduction
Burgeoning urbanization and steep growth of global population played a pivotal role in the energy scarcity. The depletion of fossil fuels become not a matter of just a discussion but it become a reality [1, 2]. Although the war between nations already become a nightmare, sustainability is a long-lasting slogan put forward for the betterment of human society. To resolve the non-availability of the non-renewable energy sources, the research has been directed towards the renewable energy sources [3] [4]. Renewable energy conversion technologies such as solar cells, wind turbines, wave energy, etc. become most popular choices. But their intermittent nature of energy production has become an issue in delivering power on demand in a 24x7 basis. To eradicate this issue, the electrochemical energy storage

technologies are evolved. The electrochemical energy storage technologies become popular due to their high efficiency, compact device structure, portability, low-cost and scalability. Among the various electrochemical energy storage technologies, rechargeable batteries and supercapacitors become most popular due to their excellence in energy storage, scalability and efficiency, and long cycle life. Rechargeable batteries become a viable source of energy storage due to their high specific capacity, long cycle life and portability [5, 6]. Among the various electrochemical energy storage technologies, rechargeable batteries facilitate efficient route for the management of power supply with storing electricity in the form of chemical energy with higher efficiency. Modern devices like electric vehicles, portable personal electronics, power tools and many other electronic devices depends highly on rechargeable batteries, especially the lithium-ion batteries (LIBs) in the past. But these LIBs have some disadvantages due to the increase in cost for Li-based resources and its non-uniform geographical distribution. This introduced a new research route for the post-Li battery technologies, such as metal-ion battery (for example, sodium-ion (Na-ion) battery (SIB), potassium-ion battery, etc), dual-ion battery and other battery-types, to overcome the challenges associated with LIBs [7]. Thus, LIBs are not only competing the current demand for energy storage devices, despite of its high-performance characteristics. Hence there exists a huge demand for other class of battery-type material in energy storge devices. Batteries are selected according to its several features for specific purpose like portable electronics, grid storage, portable electronics, home appliances, etc., and for the requirement such as required voltage, power density, energy density, cost, cycle life, etc [8]. LIBs are higher characteristic performance having reduced weight and it is mostly suited for portable electronic devices like mobile phone[9, 10]. In addition to this, SIBs are best suited in applications, but their weight, price and environmental concerns have higher priority, like as grid storage, where batteries are used in long durations [11, 12]. These long-term applications need higher degree of capacity in cheaper and low frequent recharging.

Developing sustainable materials for rechargeable batteries become highly demanding due to the versatility of the devices for modern electronic devices[13, 14]. Environmental acceptability become mandatory for all the newly emerging technologies and devices on par with the Sustainable Development Goals (SDGs) put forwarded by United Nations [15]. The basic entity for any device is material hence developing a sustainable material for any device is the basic step. The salient features of materials such as sustainability, recyclability, availability, energy efficiency, etc. play a crucial role in their wide acceptance. In the case of emerging rechargeable batteries such as post-LIBs, which mainly focus on the non-Li electrodes [16]. The reduction in cost, sustainability and material abundance are the most astonishing features expecting from a non-Li electrode for application in rechargeable batteries [17]. A statistical analysis on number of publications based on rechargeable batteries for the past 20 years are given in **Figure 1**. From this statistical analysis, it is clear that rechargeable batteries become utmost interest for the mankind due to its efficiency to compete the current energy demand.

The recent developments in the flexible and wearable electronic devices, flexibility become the heart. In the case of modern energy storage technologies, the major parameter for their practical applications lies in their flexibility. Flexible electronics is a highly flourished research area in the past decade with historical breakthroughs. It is found that this flexible electronics field have wider applications in the different aspect of human life, which includes wearable sensors for the monitoring of human behaviour pattern [18], flexible micro-mobile power in portable exoskeleton and for implantable electronics in minimally invasive surgery/pathology diagnostic medical imaging [19], remote-health monitoring [20], etc. In addition to this, synergistic combination between diverse flexible and wearable gadgetries showcases the utilization of flexible and wearable electrochemical energy storage devices such as supercapacitors and batteries [21]. The multifunctional applications in daily life and internet-

of-things (IoTs)-based microelectronic devices necessitate flexible and safe electrochemical energy storage devices to power them. Developing flexible and wearable electrochemical energy storage devices require flexible and wearable substrates to prepare electrodes for their manufacturing. The preparation of flexible substrates necessitates lightweight and good mechanical properties along with good electrochemical properties.
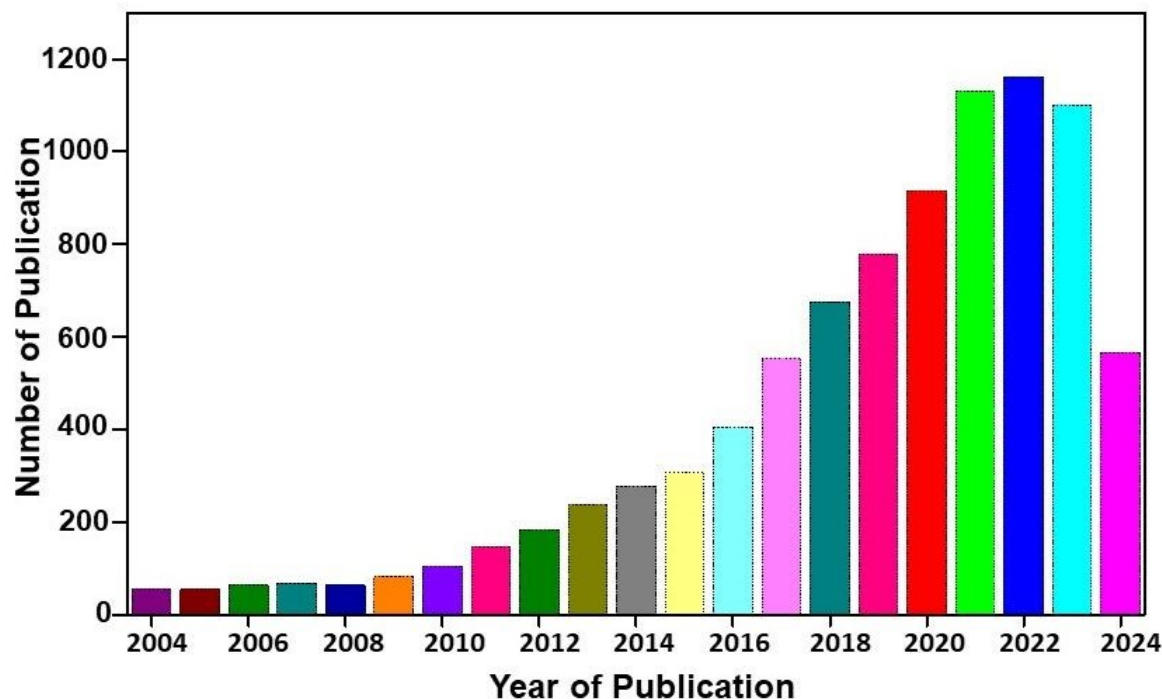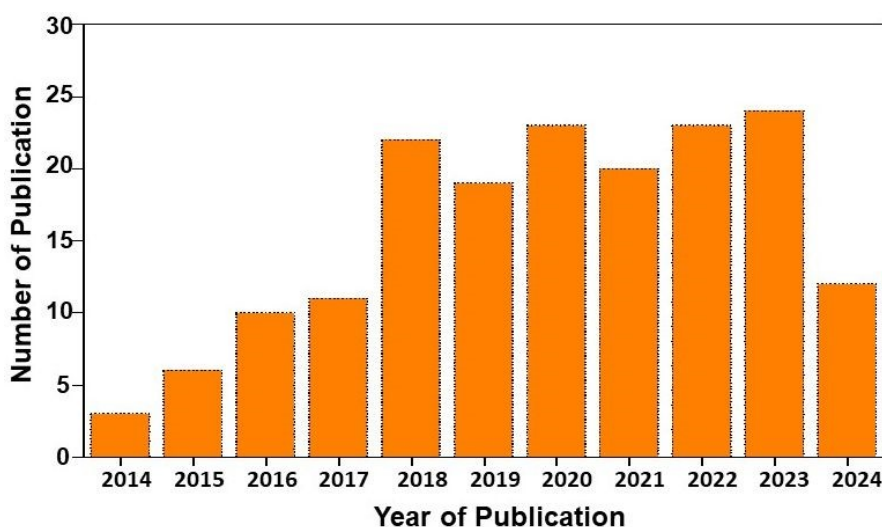


**Figure 1.** Statistical analysis of number of publications in rechargeable batteries for the past 20 years [Source: Web of Science].

The fabrication of flexible energy storage device, namely rechargeable batteries are highly depending upon the selection of suitable substrates. Modification of energy storage device on flexible substrates introduced their application in IoT based electronic devices. The fiber-based materials facilitate higher thermal conductivity, chemical stability and electrical conductivity. Carbon fiber (CF)-based materials are prominent one among this and it found application as current collector and active material for energy storage devices. Depends upon the graphitic character, CF microstructures can be completely graphitic-CF, semi graphitic-CF and non-graphitic CF. Directional orientation in these fiber-based materials especially CF hold a mesophase pitch precursor which introduce bonding of carbon-carbon conductive framework which contain pristine CF along carbonization procedure [22, 23]. CF having higher content of graphite which holds the ability to promote insertion/extraction of Li-ion into/from the graphite, which not only act as an anode for LIBs, but it provides higher capacity due to their high loading of graphite mass. CF-based electrodes are not only free-standing but also capable for the intercalation/deintercalation of cations/anions. When it is utilized as a both cathode and anode, CF-based materials are capable to forms a dual carbon CF battery. The material researchers and energy scientists are highly concentrating on the feasible application of these CF-based materials in rechargeable battery applications. A statistical analysis of number of publications in fiber-based rechargeable batteries for the past 10 years given in **Figure 2**. From the present statistical analysis, we can find that there is a limited number of publications based on rechargeable batteries with flexible CF material. The integration of rechargeable batteries to flexible electronic devices is a challenging factor. For a flexible device application, it is

3

necessary for the battery to provide adequate flexibility without degrading its charge storage performance during the operation. To achieve flexibility to the rechargeable batteries, CF can be used as a substrate/additive during the manufacturing process. By this way, a high flexibility to the flexible electronic device can be achieved by providing high bendability, and twistability required for the operation. CF-based flexible rechargeable batteries have received great attention in the recent past. But a detailed review article in this field is lacking and this has motivated us to write this article. In this review we discussed the salient features of CF-based rechargeable batteries, their preparation and electrochemical performance evaluation, which is necessary for the futuristic research related to CF-based devices with high flexibility during the operation. Hence, this review stands alone in the field of CF-based rechargeable batteries in the literature. A glimpse on the content of the present review is given in **Figure 3**.



**Figure 2.** Statistical analysis of number of publications in fibers-based rechargeable batteries [Source: Web of Science].

4
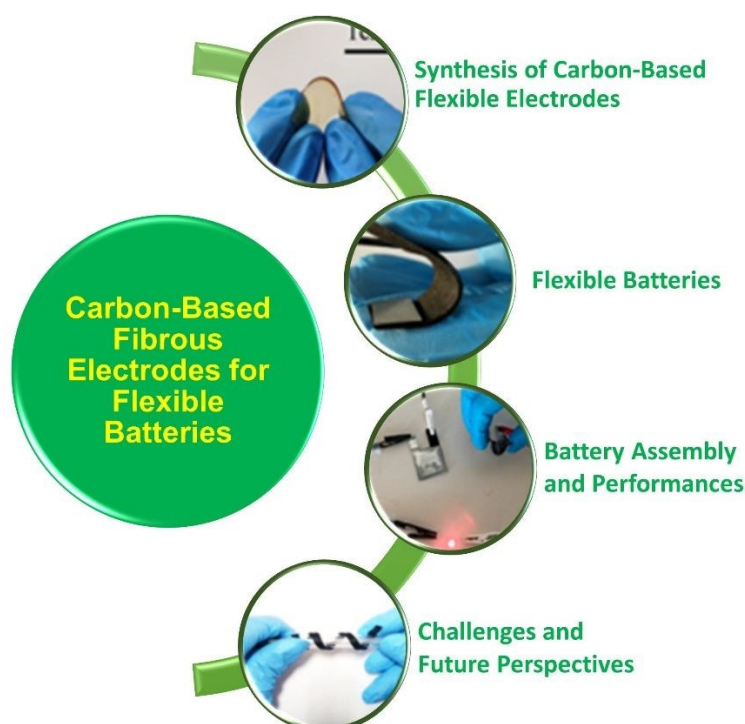
**Figure 3.** Contents of the present review.

## 2. Synthesis of Carbon-Based Flexible Fibrous Electrodes for Rechargeable Batteries

Synthesis of CF having defined morphology and architecture have prominent interest in the fabrication of rechargeable batteries. A schematic representation of synthesis methods used in CF-based flexible electrodes are shown in **Figure 4**. Here the present section depicts the synthesis methods established for CF-based materials.
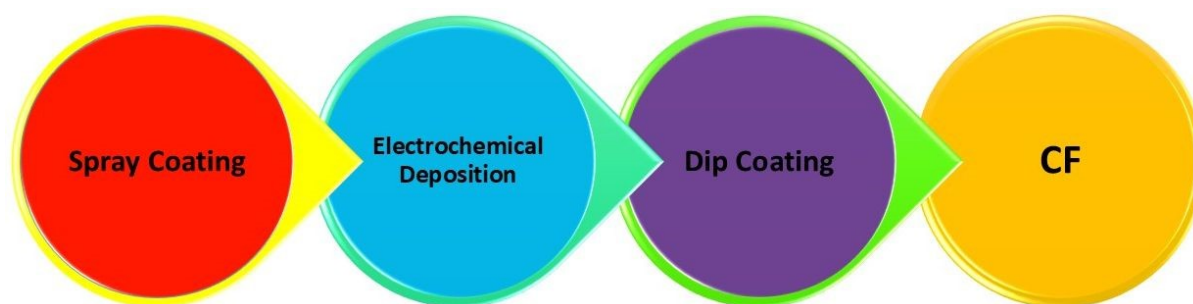


**Figure 4:** Synthesis methods of CF-based flexible electrodes for rechargeable batteries.

### 2.1 Synthesis of Flexible Electrodes by Spray Coating

One of the major limitations in development of structural batteries underlying with the requirement of positive electrode components. To develop batteries, which completely based on CF, it is imperative to demonstrate the cathode active material to these CFs. This necessitates the perfect coating of each of the individual fiber, which aims to optimize the lightweight CF utilization and facilitate transition from the micron to macroscopic scale application in rechargeable battery. In accordance this necessity, there are so much of studies are established to design a prominent technique for the synthesis of CF. In this perspective, spray coating is found to be an efficient route for the coating/synthesis of CF electrode materials for rechargeable battery application. The spray coating process provide feasibility to deposit thick film for improving surface components taken from various class of materials. In spray coating approach it only needs less amount of chemicals, having fewer steps for the procedure, thereby it produces reduced amount of waste during this synthesis. There is a report which establishes the spray coating technique of LiFePO$_4$-coated CF for structural battery demonstration. A schematic representation of spray coating apparatus is given in **Figure 5**. Here, 24K polyacrylonitrile (PAN)-derived CFs type IMS65 was distributed manually and affixed in a 2 cm × 4 cm Kapton frame for easy handling. This given frame was positioned over a hot plate, fixed at a temperature of 100ºC. Here spray gun of the apparatus was affixed in a holder which is positioned in a height of 8 cm above the CF samples, which ensuring comprehensive coverage of total fiber surface. This spraying procedure was proceeded in an ambient environment condition. The gun is connected to nitrogen inlet, which provides flow from the reservoir to nozzle. The slurry for electrode is loaded into spray gun reservoir and an equal quantity of slurry was applied to both side of CFs. A specific time interval; is introduced during spraying process to allows the evaporation of solvent (N-Methyl Pyrrolidone) and to settle solid particles on CF surface. For a spray coating procedure, it is necessary to ensure adhesion of sprayed particles on CF surface in a proper manner. During continuous spraying, particles which are already deposited over CF may dislodged, before give a chance to

RSC Sustainability Accepted Manuscript

completely adhere. Hence the continuous spraying is found to be detrimental to control the homogeneity and thickness of the coating. Hence, the spraying process is performing in a batch by batch process, which allows evaporation of carrier solvent and the particles to settle over the CF substrate. Mainly due to higher boiling point value of NMP and its reduced evaporation rate, there requires an ample time during coating procedure for the sample to settle over CFs. The major disadvantages underlying with spray coating approach is the porosity in coating, because these spaces make liquid or air pass through these. In addition to this, there exists a limited control in its thickness, it remains a hurdle to tune the CF structure.
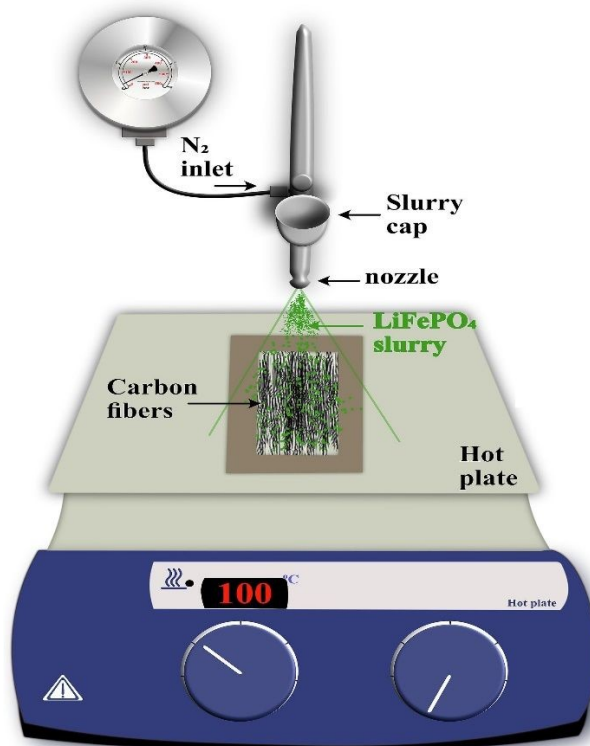
**Figure 5.** Spray-coating procedure set-up. Reproduced with permission from [24] Copyright (2024) Elsevier Inc.

## 2.2 Synthesis of Flexible Electrodes by Electrochemical Deposition

Electrochemical deposition involves the coating of a layer of material over a substrate, by the donation of electrons to the ions in a solution. The electrochemical deposition procedure is promising method to prepare coatings, and it is widely using in the case of pure form of commercial Ti, Ti–6Al–4V and CF-reinforced carbon composite. Electrochemical deposition approach possesses properties such as reduction in quantity of waste material production, low cost and easy scalability of equipment's used. In addition to this, through the change in optimization parameters, we can tailor crucial parameters in coating process such as morphology, roughness, thickness, etc[25]. The implementation of this method for these materials are due to its moderate performance condition, easy way of operation, reduced instrumentation cost and control in process parameters. Control in thickness, structure of coating and chemical constitution results to excellent performance characteristics to the prepared fibers. There is a report based on coating of nano-hydroxyapatite (HA) having favourable thickness and morphology on the surface of CF. Here mixed solution of hydrochloric acid, nitric acid, hydrogen peroxide and sulfuric acid was taken for preparation. The coating is fabricated through the combination of these mixed solution and electrochemical

deposition. In the present study, CF was fabricated from polyacrylonitrile precursor by carbonization process. In the chemical treatment, CFs are initially cleaned through ultrasonication and sequentially with acetone, alcohol and distilled water at room temperature. After that, the cleaned CFs are divided to four groups of similar mass in order determine influence by various CF treatment over HA deposition. Creating higher quantity of functional groups over CF surface is important to introduce nucleation and growth of CaP coating over fibers by interfacial chemical bond. If higher the density value of surface functional group, larger the probability to surface reaction and it is efficient the interfacial chemical bonding present between coating and fiber surface. From the FESEM imaging, the authors of present work observed that the surface of untreated CF was smooth without any apparent pitting. On the other hand, surfaces of CF obtained to be rough and pitting after treatment. In addition to this, the groves present over surface of this treated CF was wider in compared to untreated one. The proposed results shows that there exists an increase in surface area value of this treated CF. This structure hold by CF is highly related with their activity. Thereby, it is observed that electrochemical deposition is an efficient method for CF fibers to improve their activity in multifunctional applications [26]. In addition to these advantages, the major demerit underlying with the application of this route for CF fabrication is their expensive nature and dependency to environmental conditions. The utilization of toxic plating solutions are also stand as a demerit in their widespread application[27].

## 2.3 Synthesis of Flexible Electrodes by Dip-Coating

Dip-coating is an efficient route to prepare CF-based electrodes, due to their facile nature and economic feasibility in compared to other parallel routes. This is a widely used approach to prepare CF for many applications, especially in rechargeable batteries. Through dip-coating process it is possible to establish a mass production of electrode materials in an easy, scalable and reproducible way. A simple formation mechanism for film through dip-coating facilitates tunability in morphology and thickness of prepared films without any hurdle experimental set-up[28]. There is a report which based upon the fabrication of CF through dip-coating process by the method of slurry immersion [29]. For this proposed procedure of development, there is a batch of procedures which applied to continuously spooled fiber. Here torsion spring pairs having about 130 mm (~5 inches) was cut and bent at right angle about center. Aluminium cylinders with diameter of 12.7 mm (~0.5 inches) and length are prepared having two radial holes were drilled for each, which matches with two radial holes drilled for each. These holes are matching the diameter of torsion springs. Torsion springs are bonded to cylindrical ends having small quantity of 3 M 2216 epoxy with completed tensioner matching (**Figure 6a**). Each of the spring tensioner is perfectly cleaned in prior to its initial use and it is subsequently reuse for removing adhered slurry material. In this study, a series of CF samples were prepared through cutting tows having length of 280 mm and it's clasped by 3 M 2216 epoxy for the creation of circular loop, as given in **Figure 6b**. Here, the specimen's diameter is measured to be about mean value of 65 mm in diameter after performing cutting. The CF cured specimen loops are placed onto CF low tension tool, which cause torsion spring for compression for providing tension to fiber specimen. It is most prior that there is a maintenance of tow width and it is centered between torsion springs on either side of aluminium ends for avoiding contact between torsion springs. It is very important that specimen is placed in such a way that epoxy clasp not exposed to cathode slurry, which matches position as given in **Figure 6c**. The low-tension CF tool provides about 4-5 pound of force to fiber loop when it is compressed, which depends upon deviation on synthesized specimen diameter. Immediately before initiating the coating procedure, cathode slurry is removed from stirring plate and it is deposited into machined aluminium trough, given in **Figure 6d**. This provides enough liquid for the completion of submerging the sample. Then, each of this CF specimen is submerged into

cathodic slurry for a duration of 3 minutes (**Figure 6e**), it is removed and rested in inverted position (**Figure 6f**). Each of this specimen is kept for pre-dry in room temperature for a duration of 3 h and it is transferred to benchtop vacuum dry oven at a temperature of 50ºC for 12 h in order to dry. Specimens are supported in a way that CF become horizontal completely in entire drying process. Beyond the advantageous hold by dip-coating process for film preparation, it possesses a major drawback that light parts have floating off to conveyor, thereby there exists a variation in film thickness from top to the bottom portion. Also, a fat edge present in bottom of part when the excess amount of coating show lost and solvent vapour make reflux over tank removing some of their coating[30].
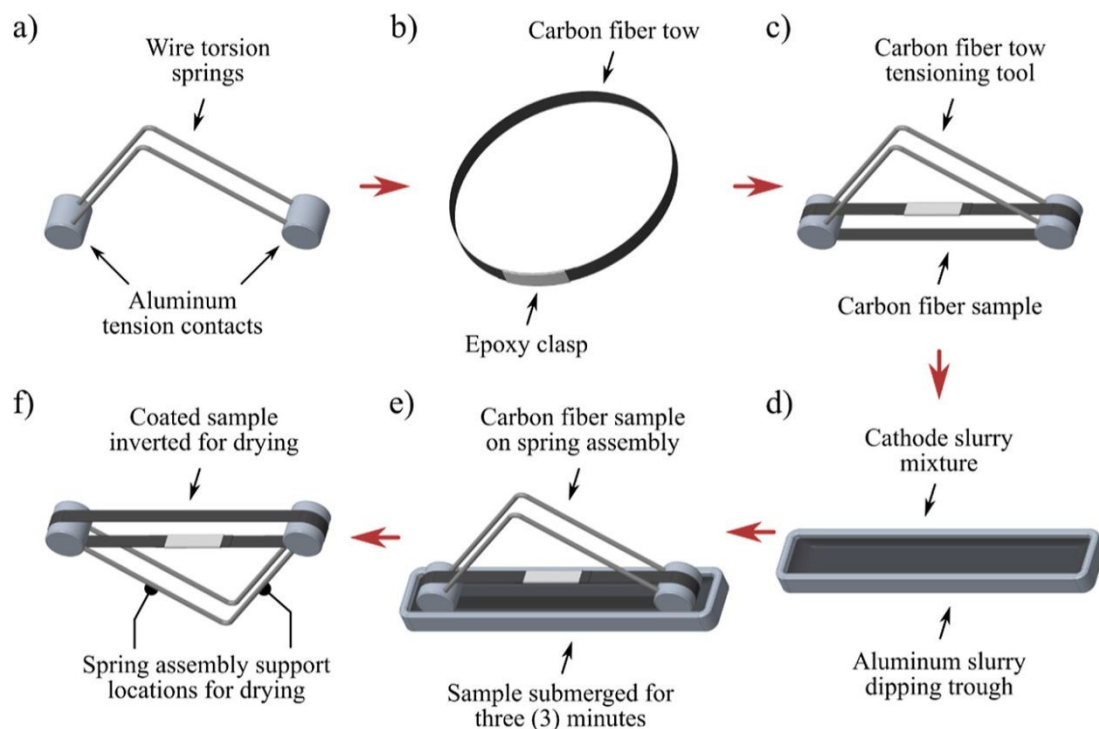


**Figure 6.** Illustration of various stages in coating process of CF cathode; a) assembling of fiber torsion tool with wire torsion spring and aluminium tension contact, b) fiber tow of sample cut and clasped by epoxy, c) fiber sample positioned over spring tensioner after cured the epoxy, d) slurry mixture of cathode mixed poured into aluminium through dipping, e) sample of fiber tow submerged into cathode slurry and f) spring tensioner fiber tow inverted to drying. Reproduced with permission from [29] Copyright (2022) American Chemical Society.

## 3. Electrochemical Performance Evaluation of Carbon-Based Flexible Fibrous Electrodes for Rechargeable Batteries

Rechargeable batteries or secondary cells are those electrochemical energy storage systems, which are capable to charge and discharge multiple times during its operation. They have achieved great attention in the recent past due to their salient features such as mobility, light weight, low-cost, high performance, etc. to name a few. Developments in the area of portable electronic device and flexible derivable introduced the higher demand for the evolution in rechargeable batteries which possess higher energy and power density, flexibility and security. The given strategies are can't fully achieved by LIB, their energy density is restricted by lithium capacity for longer applications. These batteries are delivering a theoretical capacity of 120-320 mAh/g. To modify the energy density of these devices Yin et al. [31] proposed that elements in group 16, such as sulfur (S), oxygen (O), selenium (Se) and tellurium (Te) can be

able to use as a cathode for rechargeable batteries. In this present study they prepared Te nanorods by chemical vapour deposition (CVD) on CF film, and they assembled it directly into the solid-state Li-Te batteries which contains solvent-free solid electrolyte of $LiPF_6$ dissolved in the mixture of ethylene carbonate (EC) and dimethyl carbonate in a ratio of 1:1. From the SEM images they found that Te is grown from CF and the inner diameter and wall thickness of Te nanotube is about 60 nm and 20 nm, respectively. The fabricated flexible Li-Te battery delivered a higher gravimetric capacity of 273 mAh/g and volumetric capacity of 1707 $mAh/cm^3$ after 500 cycles in a current density of 100 mA/g. This device delivered good flexibility, security and efficient electrochemical performance. Rapid diminishing of fossil fuels and environmental considerations introduced demonstration in new generation energy storage and conversion technologies. Within this technologies, rechargeable metal air batteries got significant progress due to its environmentally friendly features, reduced cost, large energy density and safer operation. But the performance of this metal air batteries is diminished by sluggish kinetics introduced by oxygen evolution reaction (OER) and oxygen reduction reaction (ORR). Among various materials, platinum (Pt) based materials are catalyses the ORR reaction strongly and ruthenium (Ru) or iridium (Ir) materials are introducing OER. But catalysts have higher cost, reduced stability and lower earth abundance limiting their application in metal-air batteries. Also, these catalysts have single catalytic performance either as an ORR or OER. There are large number of researches was conducted to develop non-precious metal electrocatalysts, like heteroatom-doped carbon catalysts and transition-metal based catalysts. Transition-metal based catalysts have problems such as reduced conductivity and degradation by the dissolution of metals.

Currently carbon-based electrocatalysts with heteroatom doped are free from metal, possess lower cost and higher stability are widely discussed. From the experimental findings and theoretical calculation, it is found that introduction of heteroatoms like B, F, P, S and N into carbon matrix which can improve the ORR and OER activity by the polarization and alteration of spin density of nearby carbon atoms. This introducing catalytically active sites which will promotes adsorption/desorption of oxygen. Based upon these facts, Wang et al. [32] synthesized B, N and F-tri-doped lignin-based CFs (BNF-LCFs) through electrospinning, pre-oxidation and carbonization with biomass lignin as source of carbon precursor and PVP as a spinning additive, zinc borate as boron source, ammonium fluoride as source of fluoride and as a partial nitrogen resource. The route is found to be simpler, efficient and eco-friendly. They found that zinc borate and ammonium fluoride addition is not successfully make doping of B and F sources, but it was increasing the amount of N and defect degree in carbon matrix. Here zinc borate is producing large number of pores and introducing higher surface area which holds large active sites. Their experimental studies reveal that the prepared BNF-LCFs is possess fascinating ORR and OER catalytic activity and stability for electrochemical reaction. The assembled liquid ZAB consists of BNF-LCFs have larger specific capacity of 791.5 mAh/g and good cyclic stability which is obtained to be higher than the value obtained for $Pt/CF+RuO_2$. Due to the efficient flexibility of BNF-LCFs, the fabricated ZIBs have good electrochemical performance with efficient flexibility.

Fiber-shaped energy storage devices have received significant attention because of its reduced volume, good flexibility and easy for textile integration. But its reduced energy density is limiting their practical application in daily life applications. So, there are number of efforts are devoted to increase the energy density of these fiber-shaped energy devices. Rechargeable Ni/Fe aqueous battery is researched from last few years, especially due to its safer operation due to the absence of organic electrolytes and large ionic conductivity with higher energy density in a reduced cost. But its reduced power density and cyclic stability is stand as a demerit for its industrial application. So, the selection of an efficient high performing material is a suitable way to overcome this issue. By taking this in mind, Liu et al. [33] controlled the activity

of $\alpha$-$Fe_2O_3$ nanorods ($\alpha$-$Fe_2O_3$ NRs) superstructure by the controlled synthesis of them over CFs by changing the growth time and it act as a negative electrode without using binder. Here positive electrode is prepared in a core-shell structure where cobalt-nickel oxide ($CoNiO_2$) nanowires are used as core and nickel hydroxide nanosheets ($Ni(OH)_2$) is act as the shell. This flexible fiber shaped energy storage device is assembled using KOH-PVA gel electrolyte at a potential window of 1.6 V. The system delivers a specific capacity of 0.62 Ah/cm³, volumetric energy density of 15.47 mWh/cm³ with 228.2 mWh/cm³ at 1 A/cm³ current density. As fabricated device has cyclic stability of 90.1% after 2500 cycles with a bending angle of 180ºC. This work reveals the significance of fabrication of flexible device from CF.

## 3.1 Metal-Ion Battery

Reduced Li resources, flammability induced by organic electrolyte and reduction in electrochemical performance produced by LIBs introduced the necessity to researchers to focus their views towards other battery devices. In these perspectives, metal-ion batteries specifically zinc-ion batteries (ZIBs) have received great attention recently. But it is found that ZIBs have reduction in its electrochemical performance due to dendrite formation. So, there are number of efforts are devoted for the modification of its performance. To deals with this issue introduction of some substrates such as Ni, Cu, etc., and some additives will modify the performance. By considering this in mind, Qian et al. [34] used a simple and facile method where they electrochemically coated a zinc-philic Cu nanosheet layer on a activated carbon cloth as a flexible 3D current collector. The small size metallic Cu particles didn't make a complete wrap over CF for a deposition of 300 s. With respect to an increase in the deposition time, CF make a complete covering by Cu, which forms uniform copper layer. The authors of this work found that the as-prepared Zn with modified surfaces consists of higher amount of large-sized nanosheets, but in the case of Zn with Cu on carbon cloth surface is consists of Zn-particles with small size. Their experimental analysis shows that Cu nanosheet is reducing the nucleation of Zn, it was increasing the surface area and electronic conductivity and it leads to the deposition of Zn on a current collector in a uniform way during the charging/discharging process. Here, $MnO_2$ with activated carbon cloth was used as the cathode. The assembled flexible device has higher capacitive retention of about 94.8% and coulombic efficiency of 97.9% after 100 cycles in a current density of 1 A/g. This higher performance is delivered through higher affinity of Cu to Zn, presence of abundant active sites and uniform distribution of Cu nanosheet layer over activated carbon cloth behaves as Zn deposition seeds. Prominently, Cu nanosheet coating layer over activated carbon cloth act as a current collector and it increase the specific surface and make a reduction in nucleation hinderance of Zn. During the plating/striping procedure of Zn, the $Zn^{2+}$ initially nucleated and deposited over Cu seeds and further it grew to Zn spherical metal particles. In final stage, the Zn spheres separated are connected together and it is developed to a dense layer which covers entire anode surface. In comparison to homogeneous deposition by Zn over Cu nanosheet with activated carbon cloth, the procedure for Zn deposition during cycles is entirely different. In accordance to reduced specific surface area and small amount of deposition sites of activated carbon cloth, the deposition of Zn tends to proceed at deposition sites, which leads to uneven growth during cycles and ultimately make formation of dendrites.

## 3.2 Metal-Air Battery

Rechargeable metal-air batteries are considered as a future battery resource for multifunctional applications. Ji et al.[35] introduced a facile free-spinning strategy followed by carbonization technique in order to mass synthesize the nonprecious transition metal CNTs prepared on carbon-nanofiber films (MNO-CNT-CNFFs, M = Fe, Co, Ni). Fabrication process is given as **Figure 7(a)**. Initially, the solution consists of polyacrylonitrile (PAN), cellulose acetate (CA)

and iron (III) acetylacetonate [Fe(Acac)$_2$/Ni(Acac)$_2$] which dissolving into N,N-dimethylformamide and it act as a spinning precursor for mass synthesis the metal rich nanofiber film (M-NFF) as given as **Figure 7(b)**. The as prepared M-NFF is then stabilized at a temperature of 280ºC as given in **Figure 7(c)** after applying a carbonization treatment at a temperature of 800ºC in order to pyrolyze this stabilized M-NFF with the presence of melamine. In this process of carbonization, the melamine is introducing a underwent pyrolysis in order to produce graphitic carbon nitride and it is going to deposit on M-NFF. During this procedures CA is going to decompose by the release oxygen contain gas and it leaving the channels in carbonized PAN fibers. The introduction of these channels is producing benefits for exposing transition metal that act as a catalyst for CNTs growth and also for the creation of MNO-CNT active material. MNO-CNT-CNFF in a uniform and free-standing structure (**Figure 7(d)**) is generated after cooling down carbonized product to the room temperature.
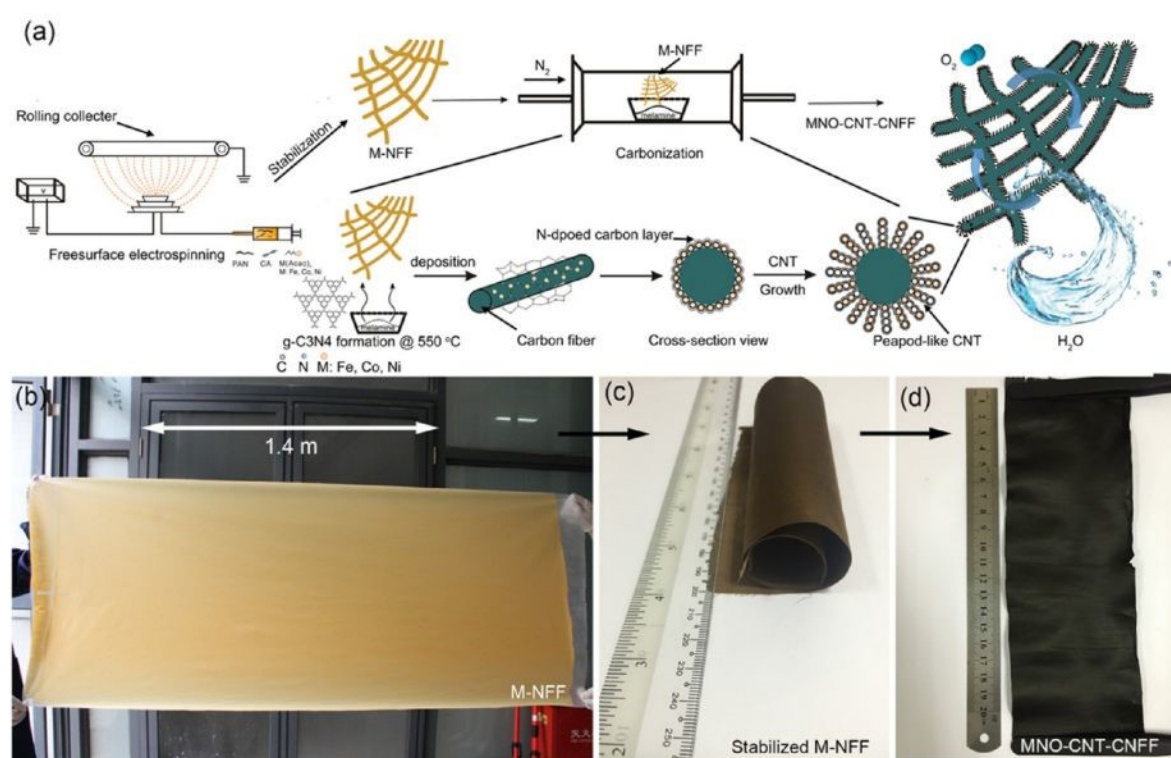


**Figure 7.** (a) Pictorial representation of fabrication process of MNO-CNT-CNFFs, (b) Mass production step of Fe-NFF by free-surface electrospinning technique in a time duration of 15min and size of the -prepared film is 180x80 cm$^2$, (c) MNFFs stabilized, (d) prepared MNO-CNT-CNFFs getting after carbonization with melamine. Reproduced with permission from [35] Copyright (2017) American Chemical Society.

**Figure 8** gives an idea about the morphology of as synthesized MNO-CNT-CNFFs, the SEM images clearly representing the growth of Fe, Ni and Co catalysed CNTs. **Figure 8(a-c)** shows that the CFs prepared by electrospun technique is holding a diameter of 600 nm and it hold a homogenous coverage by the peapod-like structured Fe-based CNTs which are in-situ grown. These peapods have a diameter of 10-30 nm with length range of several hundred of nanometer. Well-crystallized peas having a diameter of 5-20 nm with a lattice distance of ~0.21 nm (**Figure 8e**). In agreement with the XRD pattern given as **Figure 8(f)**, the crystalline structure hold a Fe$_3$C and cubic Fe structure. TEM image **Figure 8(d)**, hold an empty and hollow pod-like structure which tends to be increasing the surface area in order to increase its catalytic activity.

In TEM image of CNT given in **Figure 8(d)** and **(e)** it shows that lattice fringes having an interplanar distance of ~0.34 nm which corresponds to the C (002) plane and it hold higher amount of exposed edge sites which improving the catalytic activity. The elemental mapping images given in **Figure 8(g-k)** represents that there exists a uniform distribution of C, O, N and Fe in synthesized material.
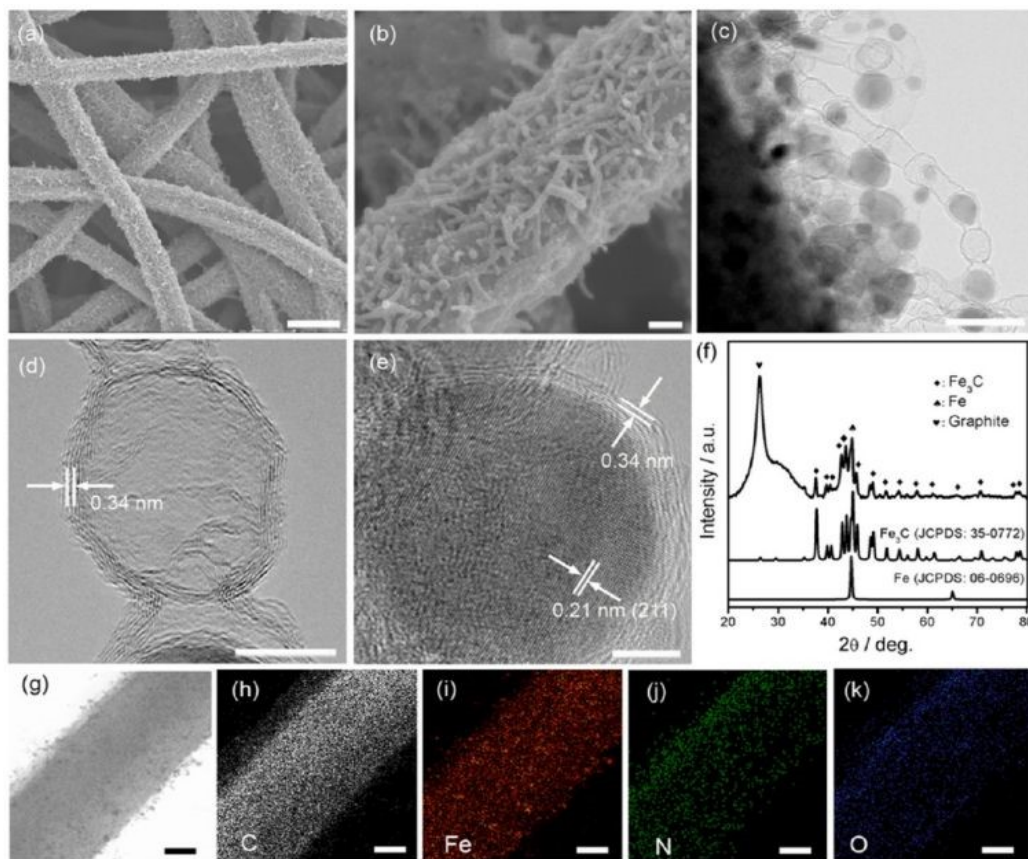


**Figure 8.** (a) and (b) SEM image of FeNO-CNT-CNFF (c-e) TEM image (f) XRD pattern of FeNO-CNT-CNFF (g-k) Elemental mapping image of C, O, Fe and N. Reproduced with permission from [35] Copyright (2017) American Chemical Society.

Due to efficient bifunctional electrocatalytic features and novel physical characteristics FeNO-CNT-CNFF melamine treated at 800°C is used as an air electrode for fabricating rechargeable hybrid Li-air batteries. Pictorial representation of rechargeable hybrid LIB consists of anode as Li metal and NASICON type $Li_{1.5}Al_{0.5}Ge_{1.5}(PO_4)_3$ (LAGP) anode protects membrane (**Figure 9a**). The constructed anode chamber is consisting of 1M $LiPF_6$ in EC-DMC to reduce the interfacial resistance. Also, 1 M LiOH aqueous solution is applied as catholyte solution. This hybrid LAB achieves a higher voltage of ~3.4 V, is used to lighten the LED to reveals its commercial application (**Figure 9b**). A comparison of charge-discharge curve of hybrid cell using various cathodes is given as **Figure 9(c)**. The fabricated battery material exhibits an effective operation with a voltage window of 0.15 V in a current density of 0.03 mA/cm², this value is smaller than the Pt/C+Ir/C air electrode. **Figure 9(d)** shows that the hybrid LAB performing stable reduction of 4e⁻ performance in different current density. **Figure 9 (e)** and **9 (f)** exhibits a stability after 21 cycles while exhibiting a specific capacity of 30 mAh/g.
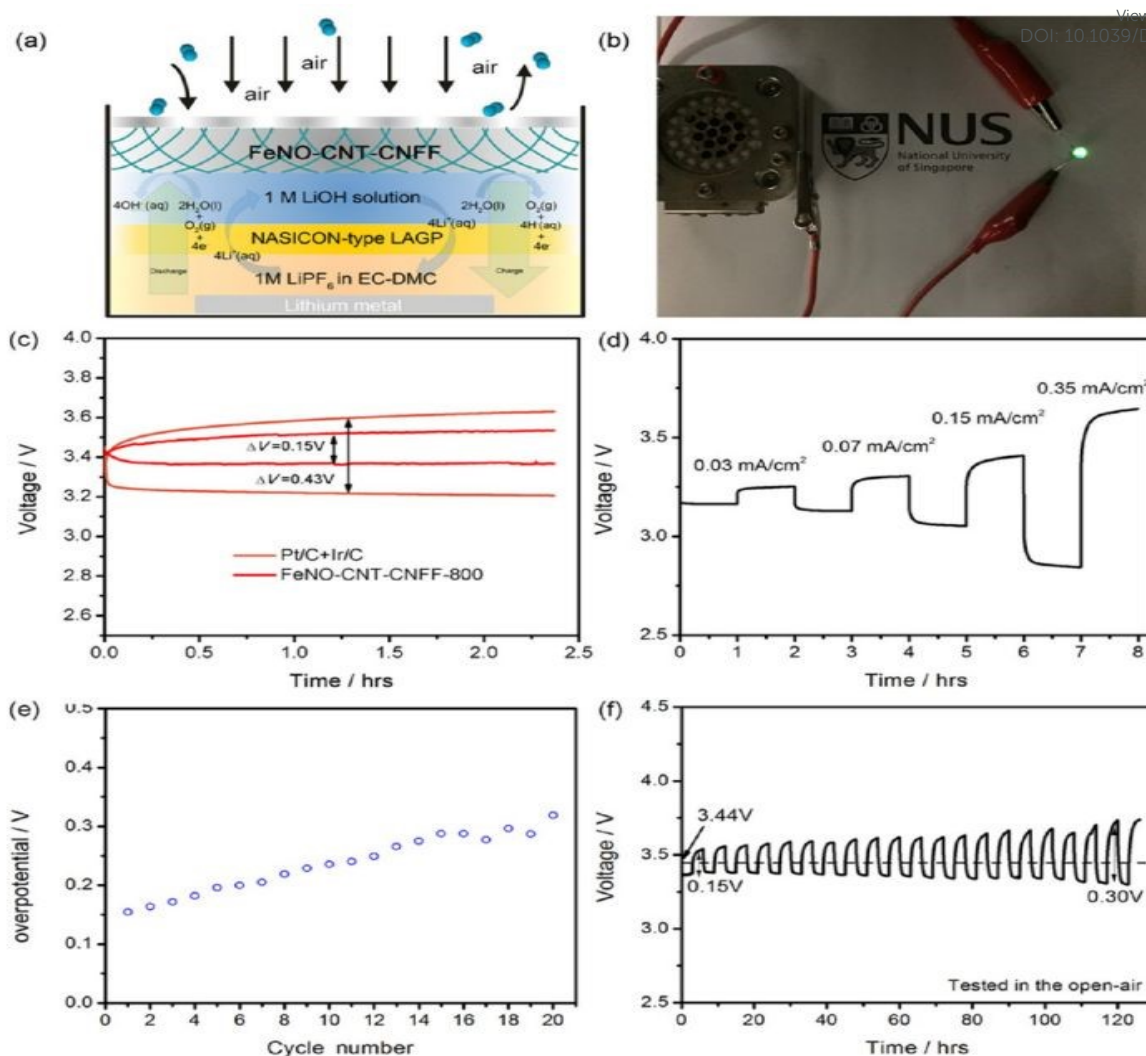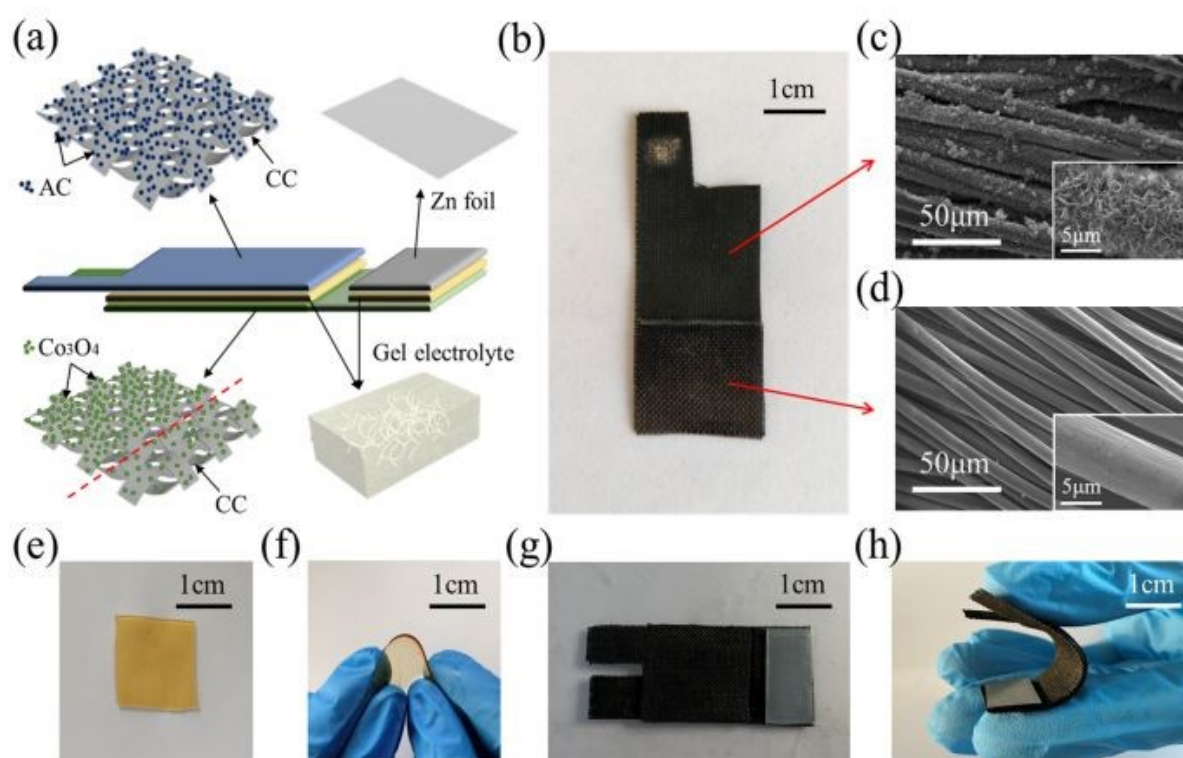
**Figure 9.** (a) Pictorial representation of rechargeable Li-air battery, (b) digital photograph of FeNO-CNT-CNFF based hybrid Li-air battery which lighting the LED, (c) Voltage gap comparison of charge-discharge voltage plateau with different catalysts for Li-air battery, (d) charge-discharge curve of as prepared LAB with various current densities, (e) change in overpotential of LAB with change in cycle number, (f) cyclic performance analysis of LAB in open-air condition. Reproduced with permission from [35] Copyright (2017) American Chemical Society.

### 3.3 Zin-Air Battery

Zinc-air battery (ZAB) is a relatively new concept in the field of rechargeable batteries. Hou et al. [36] fabricated hybrid energy device composed of rechargeable ZAB with asymmetric supercapacitor constructed on carbon cloth (CC) film. Here, the nanostructured $Co_3PO_4$ grown on carbon cloth by electrochemical deposition in a constant voltage method. Here the electrochemical deposition approach is utilized because this procedure establishing a uniform distribution of $Co_3PO_4$ nanostructures over CC. An overall arrangement of both devices in a sandwich-like structure is given as **Figure 10(a)**. In this arrangement the $Co_3PO_4$/CC is acted as positive electrode, KOH/PVA as gel electrolyte, and activated carbon (AC)/CC composite was used to fabricate the asymmetric supercapacitor portion and $Co_3PO_4$/CC nanocomposite as air electrode, KOH/PVA gel electrolyte and Zn foil as negative electrode is constructing the ZAB portion. With the microscopic view of constructed system (**Figure 10(b)**), it is clear that

a distinct boundary line is existing over CC possessing a highly dense black colour represents the higher amount of load of $Co_3PO_4$ and light colour shows the low load percentage of $Co_3PO_4$. From the SEM images, it was observed that higher percentage of $Co_3PO_4$ loading introducing the generation of vertically sprouting nanopetals and clusters that make a uniform distribution over the CF surface (**Figure 10(c)**) and the lower quantity of $Co_3PO_4$ loading is producing ultrathin nanocoating which wrapping uniformly over the surface of CFs (**Figure 10(d)**). **Figure 10(e)** represents the introduction of a solid-state gel and **Figure 10(f)** shows the flexibility of these film. As prepared gel electrolyte is bonding with both the positive and negative electrode as a solid-state integrated system (**Figure 10(g)**). Due to the presence of this gel electrode the assembled hybrid system also shows efficient flexibility (**Figure 10(h)**).



**Figure 10.** (a) Pictorial representation of solid-state integrated hybrid energy system, (b) digital picture of $Co_3PO_4$/CC nanocomposite. SEM image representing (c) higher loading amount of $Co_3PO_4$ nanopetals over CF film, (d) lower loading of $Co_3PO_4$ nano-coatings over CF for the ZAB part. Images showing the (e) KOH/PVA gel electrolyte film retaining water, (f) its flexible state, (g) top view of integrated device, (h) state of its flexibility. Reproduced with permission from [36]. Copyright (2021) American Chemical Society.

They analysed performance of hybrid energy system, **Figure 11(a)** describing the equivalent circuit diagram, that gives the idea about mode of operation of hybrid energy system. Here the single-pole double throw switch was utilized for achieving the instant switch of performance by the in-situ charging from asymmetric supercapacitor to its external power source. In the asymmetric supercapacitor part, the voltage is initially increasing up to 1.0 V in few seconds and then it approaches to a value of 1.15 V after 200 s of charging. During the in-situ charging process, the chemical energy which was originated from the ZAB is converted to electrical energy and it is going to store in asymmetric supercapacitor portion in a slow step process (**Figure 11(b)**). An external performance of pulse formed was obtained at a peak discharge current of 55 mA with in a duration of 5 s (**Figure 11(c)**). Accordingly, the voltage of

asymmetric supercapacitor is drop down to 0 V shown with red curve in **Figure 11(b)**. The device gives a higher power density of 7.91 mW/cm$^2$ at output voltage of 1.15 V and a peak current of 0.055 A with an area of 8 cm$^{-2}$. A comparison of change in voltage of asymmetric supercapacitor and ZAB in the cycles 1, 25 and 50 cycle is given. The output working voltage in ZAB is found to be stable at 1.17 V in the first cycle, then it drops down to 1.13 V in the 25$^{th}$ cycle, and it reaches towards 1.0 V in the 50$^{th}$ cycle (**Figure 11(d)**). A comparison of maximum voltage achieved by the asymmetric supercapacitor is given as **Figure 11(e)**, which produced by the in-situ charging process carried out in 200 s during first and second inner cycle. The selection of a proper electrocatalysts which can catalyse ORR and OER is given prior importance for the fabrication of metal-air batteries.

### 3.4 Flexible CF Battery
By considering the demand for the fabrication of flexible battery systems, Pendashteh et al.[37] fabricated a self-standing air-cathode based on macroscopic CNT fibers (CNTfs) prepared by CVD spinning follows by a hydrothermal method. Electrocatalytic activity of the prepared fibers are optimized by the tuning of nitrogen doping and defect density which can be adjusted with the hydrothermal temperature. TEM image given in (**Figure 12a**) shows that fibers are consists of interconnected CNTs, which possess a crystalline multiwalled structure with 3-5 layers and having a diameter below 10 nm as given as inset. The XPS survey spectra given as **Figure 12(b)** clearly showing the introduction of N 1s peak and the increase in intensity of O 1s peak after doing the treatment. From the inset C 1s data fitting, there exist an increase in the sp$^3$/sp$^2$ and O/C ratios, which introducing the conjugated bonds cleavage and introduction of new bond and functional group.
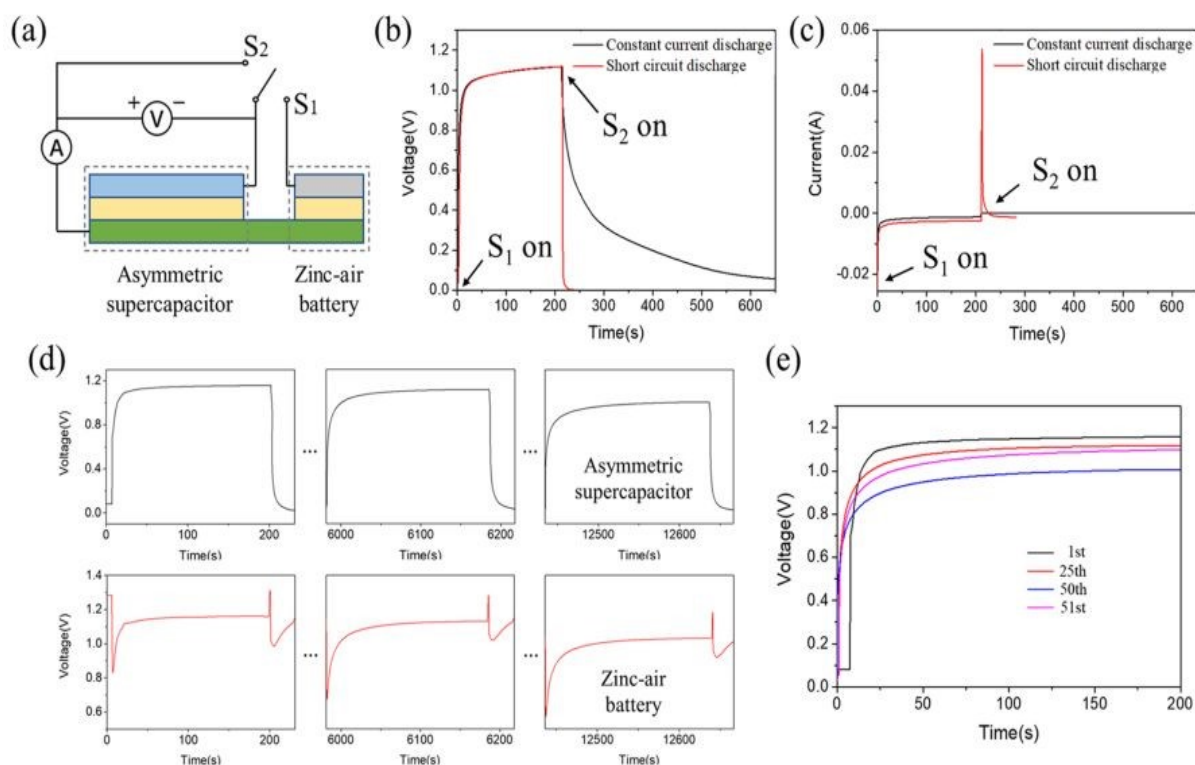


**Figure 11.** (a) Equivalent circuit of hybrid energy system, (b) Change in voltage, (c) of asymmetric supercapacitor in various constant current discharge and short circuit discharge, (d) change in voltage of asymmetric supercapacitor and zinc-air battery in 1, 25 and 50$^{th}$ cycle (e) Comparison of charge voltage curve of asymmetric supercapacitor part 1, 25 and 50$^{th}$ cycle

(within 1st inner cycle) and 51st cycle (after ZAB tends to be fully recharged and the beginning of 2nd inner cycle) in-situ operation. Reproduced with permission from [36]. Copyright (2021) American Chemical Society.

Increase in O content in maximum in the sample synthesized at a temperature of 170ºC, introduced by the functional groups adsorbed and it producing a redistribution of charges in the adjacent carbons.
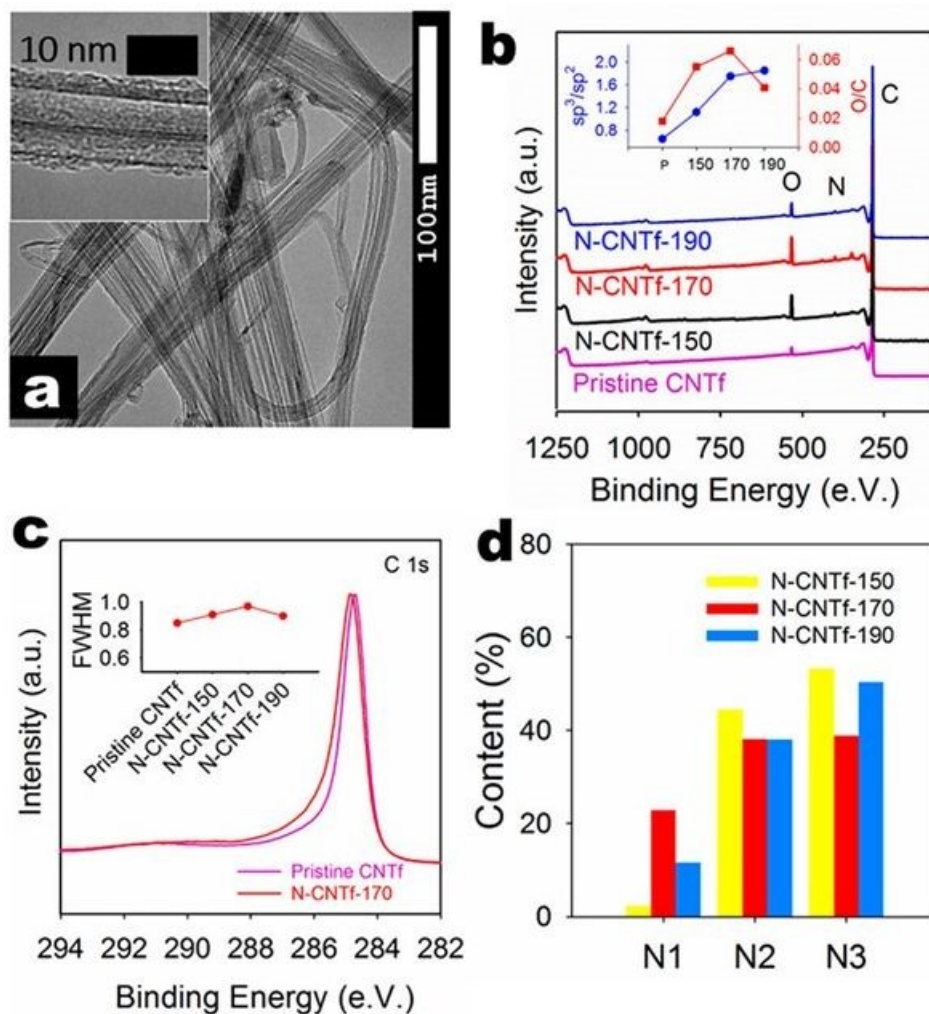
**Figure 12.** (a) TEM Image of fiber treated at 170ºC, (b) XPS survey spectra of as prepared samples, (c) C 1s spectra in high resolution for pristine and sample treated at 170ºC, (d) Core level spectra correspond to N 1s for the doped samples. Reproduced with permission from [37]. Copyright (2018) American Chemical Society.

This redistribution of charges producing an increase in intermediate species adsorption for ORR and OER which improves the catalytic property of CNTfs. There exist a shifting of C 1s line towards higher values of binding energy which agrees with the results obtained for N-doped CNTfs (**Figure 12c**). From the peak analysis diagram given as **Figure 12 (d)**, it is clear that N-doped CNTfs synthesized at 170ºC hold a higher amount of pyridinic-N atoms, it producing adsorption of oxygen atom and decomposition of hydroperoxide. Here, a ZAB is assembled using CNTf as an air cathode for liquid-based ZAB with alkaline poly(vinyl alcohol) gel electrolyte. This assembled battery shows an open circuit voltage of 1.31 V (**Figure 13**),

16

there is not less than 50 mV in ZAB. A schematic representation of battery and reaction mechanism in discharge is given in **Figure 13**, where CNT-170 catalyse the oxygen reduction reaction by 4e pathway, but Zn is oxidized and zincate species are introduced. **Figure 13** shows that charge-discharge profile of ZAB have flat voltage plateaus at the value 1.97 and 0.87 in charge and discharge respectively. It is also clear that profile didn't make any alteration in bending the cell.
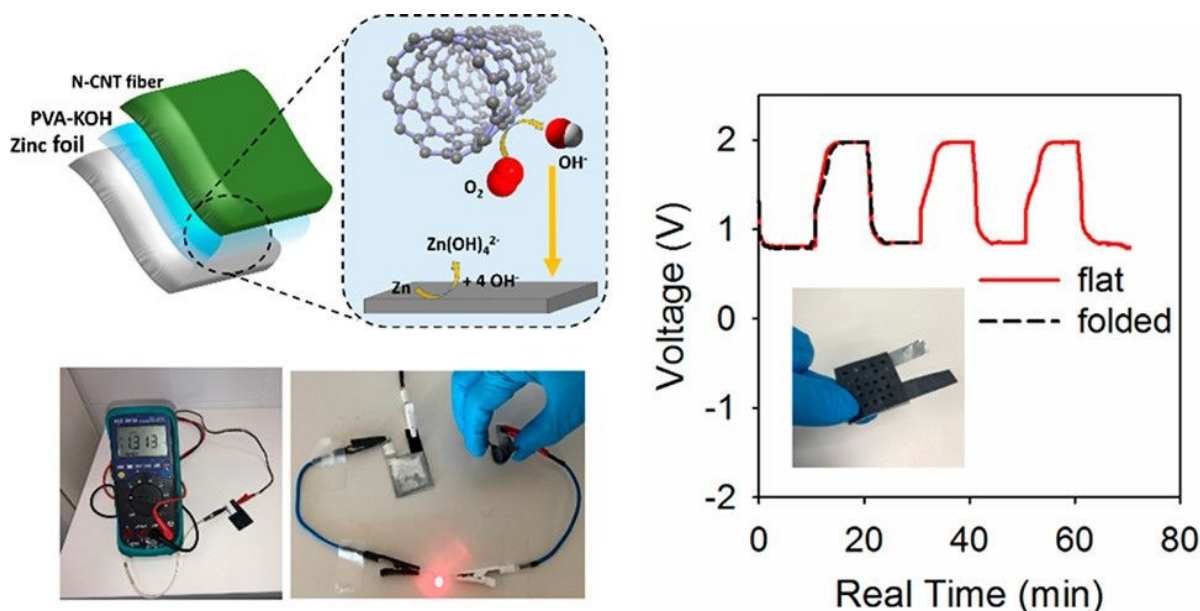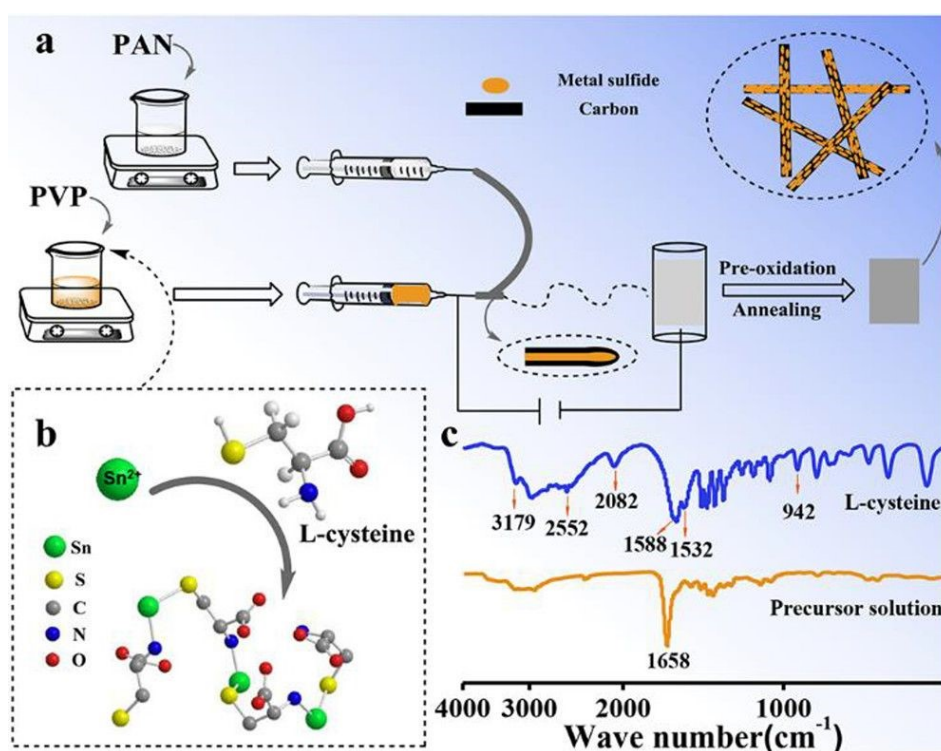


**Figure 13.** Pictorial representation of prepared rechargeable solid-state Zn–air battery with CNT fiber treated as air cathode and PVA-KOH as gel electrolyte (in the left panel). Right panel represent GCD profile of solid-state ZAB in flat and bend state. Reproduced with permission from [26]. Copyright (2018) American Chemical Society.

Due to excellent bifunctional catalytic activity of sample at 170ºC as an air cathode for liquid-based ZAB with alkaline poly(vinyl alcohol) as gel electrolyte constructed. The fabricated device shows a higher open circuit voltage of 1.31 V which is about 50 mV lower than liquid-base battery. Here the prepared electrode material is catalysing the ORR by 4e route, here the anode Zn is going to oxidize and zincate species such as $Zn(OH)_4^{2-}$ is produced. In charging process there occurs a reverse reaction and an evolution of oxygen in the CNT fibers. From the charge discharge diagram, we can able to found that there exists a flat voltage plateau in the region of 1.97 and 0.87 V in the charging and discharging process respectively. It is also found that there doesn't contain any bending of the cell. Also, there exist a red LED which is lighten by the two batteries which are connected in a series connection. It confirms the efficient performance of the prepared electrode material for the fabrication of solid device, which was formed by the defects and doping introduced in the CNT fibers. Their experimental analysis shows that the treated CNT fibers are act as an efficient tool for the fabrication of a flexible and lightweight ZABs.

Du et al. [38] fabricated a flexible electrode material of metal sulfide (SnS)@CFs by electrospinning approach, there exists an introduction of chelate complex with L-cysteine and metal cations. By considering SnS as representative material, fiber electrode with flexibility is developed by interweaving this material into CF in a continuous manner. In the half cell fabricated, Li (for SIBs, Na) acted as a counter and reference electrode. Here, 1 M $LiPF_6$ is used as the electrolyte consists of solvent of ethylene carbonate (EC) and diethyl carbonate (DEC) in a ratio of 1:1. In the case of SIB, 1M $NaClO_4$ is act as the electrolyte which consists

of solvents such as EC, DEC and propylene carbonate (PC) in a ratio of 4:2:2. Also both of these contains 5% fluoroethylene carbonate (FEC). The synthesis procedure of electrode material is given as **Figure 14(a)**. In this study, the authors choose PVP/metal salt/L-Cysteine and PAN as the precursor for core and shell layer respectively. L-cysteine have three ligands such as thiol group (R-SH), carboxyl group (R-COOH), and amino group (R-NH$_2$) which producing a bond with the metal-ion in order to create a chelate complex **Figure 14(b)**. To analyse the bonding between SnCl$_2$ and L-cysteine, FTIR spectroscopy was used. Absorption peak present at 2552 and 942 cm$^{-1}$ represents the characteristic peak of R-SH in L-cysteine and it is found to be disappearing in the SnCl$_2$ and L-cysteine mixed solution. Also, in the chelate complex the peaks 2082 and 1532 cm$^{-1}$ corresponds to R-NH$_2$ group is absent, which indicating the coordination introduced between Sn$^{2+}$ and nitrogen atom. Based upon the results obtained from FTIR, the molecular structure holds by the chelate complex is given as **Figure 14(c)**.



**Figure 14. (**a) Pictorial representation of synthesis procedure of SnS@CF by electrospinning, (b) Structure of chelate complex formed by L-cysteine and metal cation, (c) FTIR spectra of L-cysteine and mixed solution of SnCl$_2$ and L-cysteine. Reproduced with permission from [38] Copyright (2019). American Chemical Society

XRD spectrum of Uni-SnS/C prepared by the single axial electrospinning of similar solution of core-layer Coa-SnS/C is given as **Figure 15(a)**. SEM image of Uni-SnS/C and Coa-SnS/C fibers are given as **Figure 15(b)** and **(c)**, respectively. Other than a rough morphology here the fibers hold a smooth surface structure. Coa-SnS/C have a narrow range of diameter with good flexibility in the higher value of bending angle too as given as **Figure 15(d)**. From the TEM and HRTEM images given in **Figure 15(e)** and **(f)**, respectively, it is clear that the SnS is well assembled into the carbon matrix, introduced by the confinement produced by the outer layer producing the fast transfer of electron and efficient buffering through charge/discharge process. Results obtained from XRD and TEM shows that there exists an amorphous structure to the prepared electrode material which producing efficient rate capability, specific capacity and cyclic stability for SIBs and LIBs.
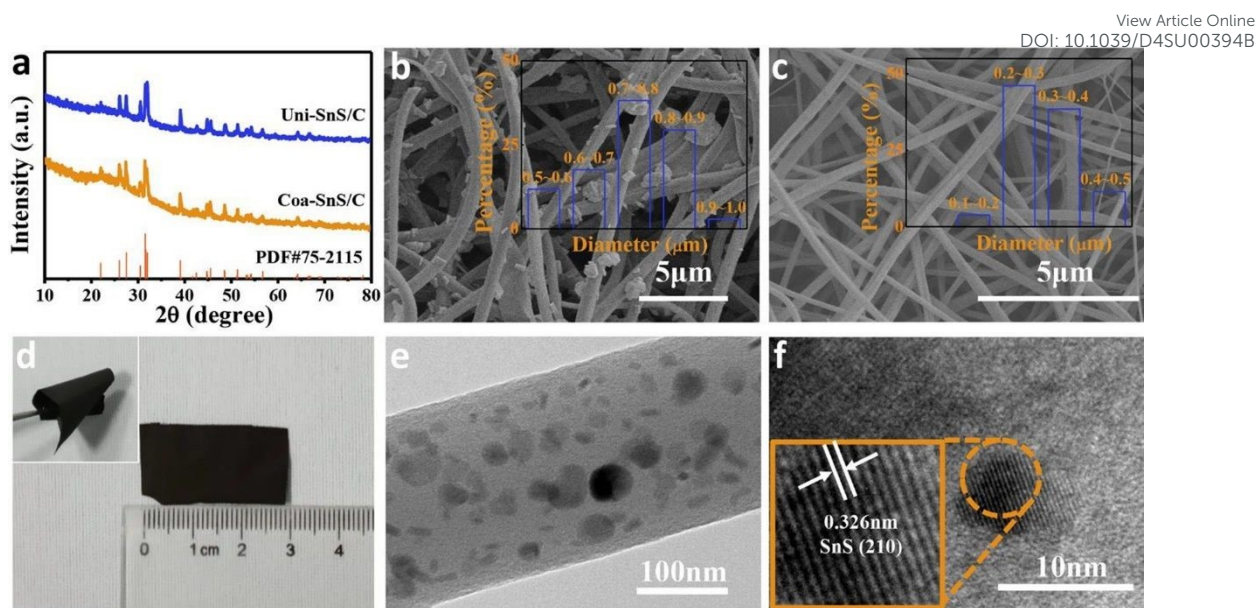
**Figure 15.** (a) XRD spectra of Uni-SnS/C and Coa-SnS/C. SEM image of (b) Uni-SnS/C, (c) Coa-SnS/C, (d) Photograph of Coa-SnS/C with higher bending angle, (e)TEM image of Coa-SnS/C, (f) HRTEM image of single Coa-SnS/C. Reproduced with permission from [38] Copyright (2019) American Chemical Society.

Li/Na storage capability of fabricated Coa-SnS/C is analysed using electrochemical study. **Figure 16(a)** represents the cyclic voltammetry (CV) diagram of Li storage. CV study was performed for first three cycles with scan rate of 0.1 mV/s within a voltage window of 0.01 to 2.5 V. During the Li storage process, in the initial cathodic scan, reduction peak originated at 1.34 V is represents process of conversion of SnS to Sn and $Li_2S$. Peak at 1.34 V is the alloying reaction between Sn and Li. In the initial anodic scan, peaks at 0.50, 0.62, 0.80, and 1.18 V corresponds to multiple step Li-Sn dealloying procedure and a wide peak at 2.0 V is the reversible conversion of Sn and $Li_2S$ to SnS phase. Like Li storage, the CV curve in Na storage consists of reduction peak corresponds to conversion and alloying reaction (**Figure 16(d)** and **(f)**). The charge/discharge curve of Coa-SnS/C with respect to Li and Na storage is given as **Figure 16(b)** and **(e)** obtained at a current density of 50 mA/g within a voltage window of 0.01 and 2.5 V. Firstly, the discharge/charge capacity attains a value of 1155.3/812.7 mAh/g for the storage of Li and 500.8/327 mAh/g for the sodium storage with a coulombic efficiency of 70.3% and 65.3%, respectively. A reduced capacity for SIB is connected with the broader and weaker CV peak for the storage of Na-ions, introduced by the sluggish kinetic of insertion and extraction of Na-ions. The rate performance of Coa-SnS/C anode for LIB is given in **Figure 16(c)**. The anode achieves a reversible capacity of 752.1, 633.4, 556.7,484, 389.7, and 317.9 mAh/g at current densities 50, 200, 500, 1000, 2000, and 5000 mA/g, respectively. It exhibited an efficient cyclic stability where the specific capacity is about 403.9 mAh/g after 400 cycles at a current density of 1 A/g and achieved a coulombic efficiency of 99.8% at 1 and 2 A/g during cycling (**Figure 16(g and h)**).
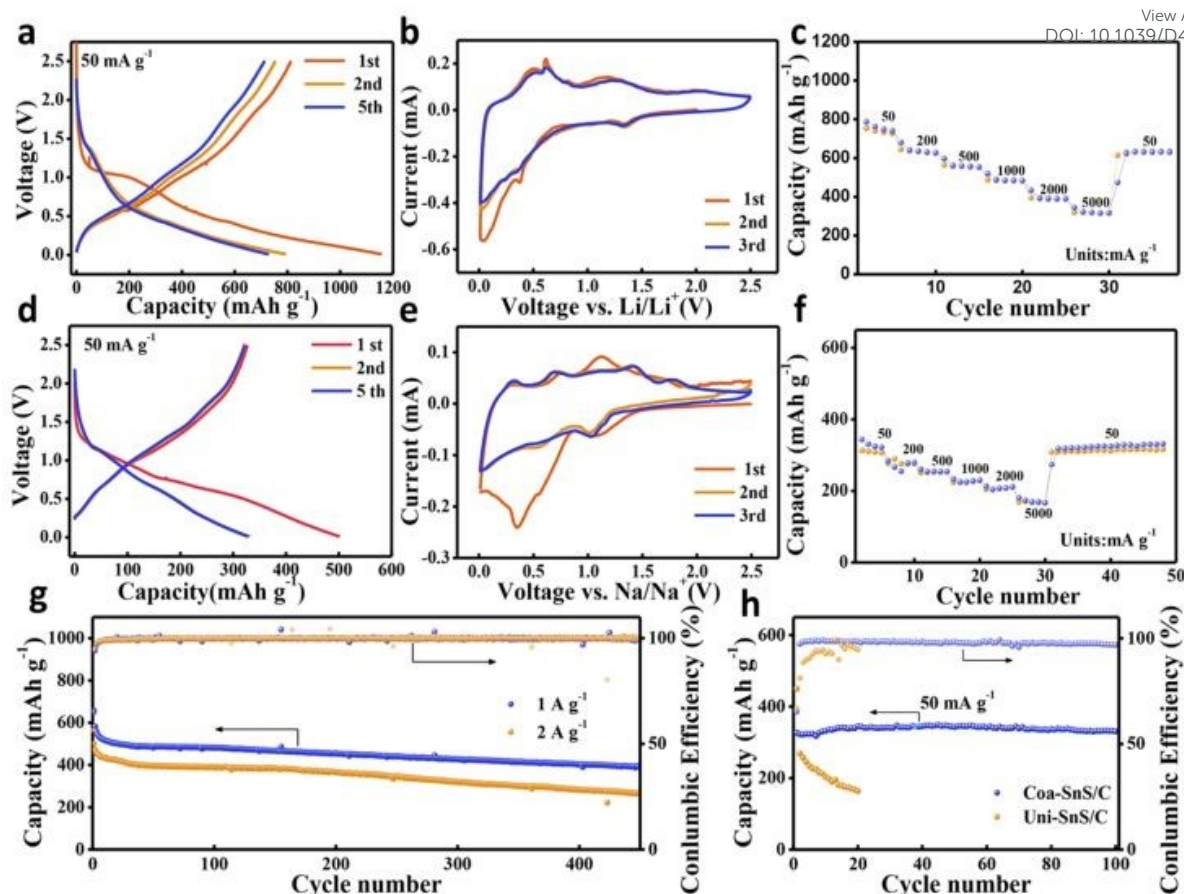
**Figure 16.** Electrochemical analysis of a-c, g for Li and d-f, h for Na (a),(c) GCD profile of Coa-SnS/C at 50 mA/g, (b) and (e) CV curve of Coa-SnS/C at 0.1 mV/s for first three cycles (c), (f) rate capability of Coa-SnS/C (g) cyclic stability evaluation of Coa-SnS/C for the storage of Li-ion at 1 A/g and 2 A/g (h) cyclic stability analysis of Uni-SnS/C and Coa-SnS/C at 50 mA/g. Reproduced with permission from [38] Copyright (2019) American Chemical Society.

In textile industries, fabrication of printable and flexible energy devices is one of the necessary things. Based upon these facts, De et al. [21] fabricated a copper-coated CF (Cu-CF) by electroless deposition route without applying any external power source for a solid state flexible battery device. This Cu-CF is employed to prepare poly(ethylene oxide) (PEO) based polymer nanocomposite is used as flexible and conductive current collector layer. Synthesis of materials for the design of solid-state battery and its fabrication procedure is given as **Figure 17**. $Cu^{2+}$ salt is going to reduce by the formaldehyde (HCHO) with the presence of NaOH and going to deposit on CFs, where the redox potential of copper is found to be highly electropositive than carbon. Then the cathodic reaction was going to continue until CFs are totally covered by Cu. To make a compromise to the reduction of adhesion introduced during coating of CFs, a less amount of benzonitrozole is added. By the copper deposition, potential involved in the potential is lower than +0.337 V, where copper ions are found to be thermodynamically stable when the potential is above this value in acidic medium. Electrochemical performance of battery is analysed by using open circuit voltage (OCV) and charge-discharge cycles as given as **Figure 18a**. Before starting the OCV analysis, the batteries are going to fully charging at a current of 0.040 mA. OCV measurements are done up to 100 min with Al foil as electron collector on anode, and value reaches to 2.67 V as given as **Figure 18(b)**. The OCV value is 0.67 V only in the absence of electron collector within anode side.
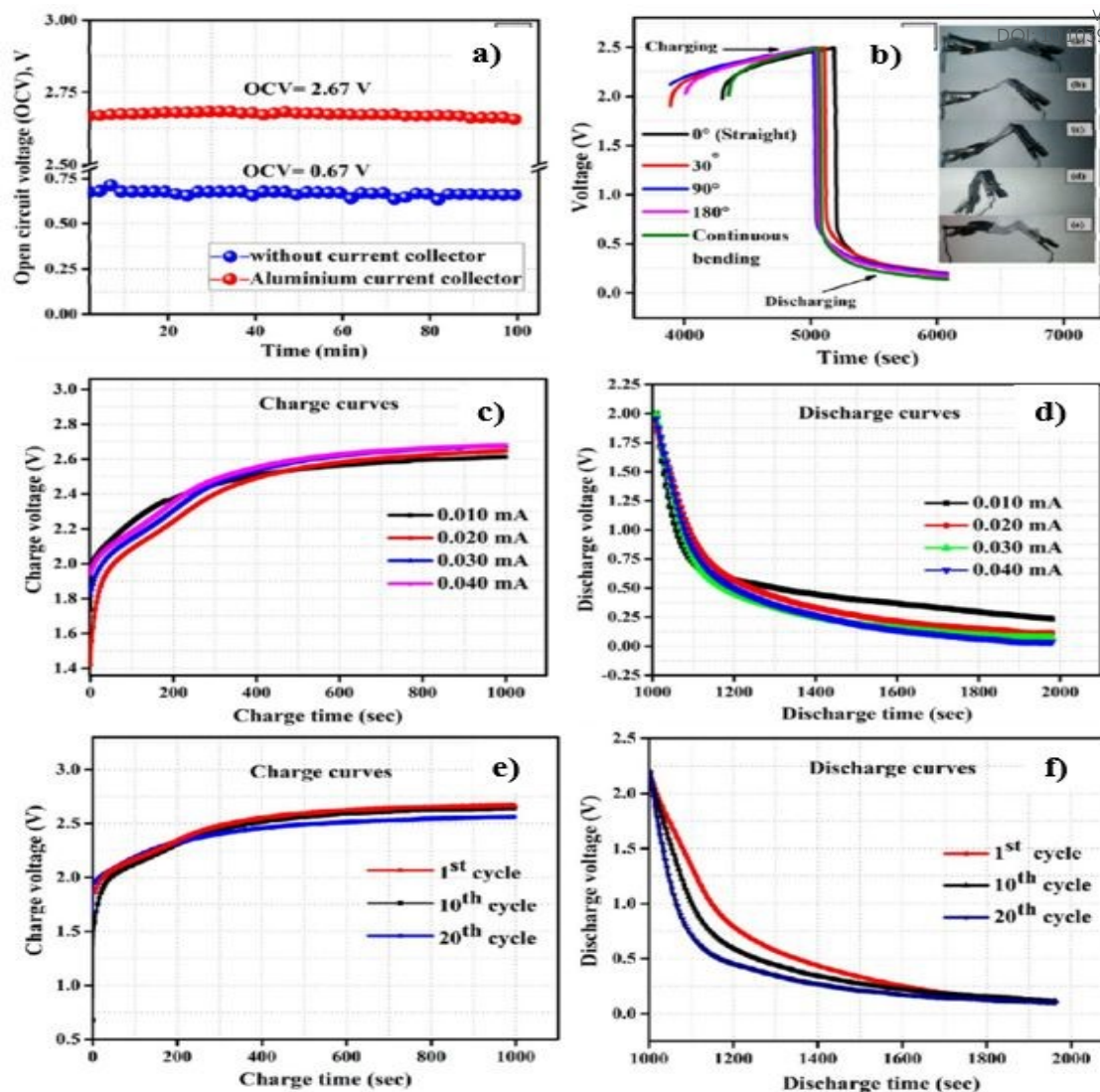
Charge-discharge curve of batteries in a repeatable bending (where folding and unfolding is done) at various angles of 30-180º is measured in order to calculate its flexibility. The charging cycles at a constant current of 0.01, 0.02, 0.03, and 0.04 mA for 1000 s, where the charging is initiated from ~1.6-2 V (**Figure 18(c)**). The charge curve with current 0.01 mA reached to a maximum voltage value of 2.62 V. By reducing the charge current applied, the voltage is reducing in a fixed charge time. The highest voltage obtained for 0.04 mA is 2.66 V and it is also found in the discharge cycle given as **Figure 18(d).**
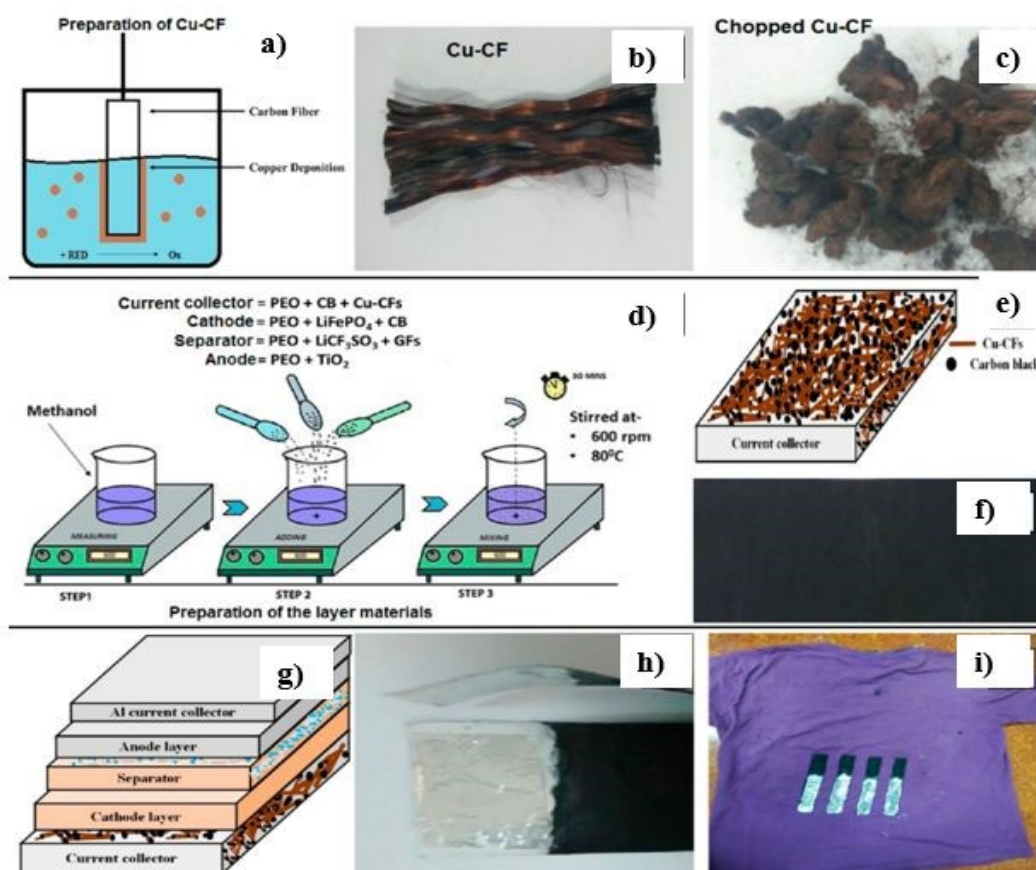


**Figure 17.** (a) Procedure for electroless deposition of Cu-CFs. Image of (b) Cu-CFs (c) chopped Cu-CFs (d) diagrammatic representation of fabrication of electrode, electrolyte and current collector layer. Current collector layer (e) pictorial representation (f) digital image g) diagrammatic representation of flexible fabric battery consists of component layer (h) and (i) digital image of battery coated over fabric. Reproduced with permission from [21]. Copyright (2017) American Chemical Society.

Charge-discharge curve at various cycles is given as **Figure 18 (e)** and **18 (f)**. **Figure 18(e)** shows that the voltage drops obtained between $1^{st}$ and $10^{th}$ cycle is about 0.02V and it is raises to 0.08V after $10^{th}$ and $20^{th}$ cycle. **Figure 18f** shows the discharge curve of $1^{st}$, $10^{th}$ and $20^{th}$ cycles, here all the curves are exhibiting similar discharge time. It is by the efficient retention in integrity in structure of battery for electrochemical operation.

**Figure 18.** (a) Analysis of OCV of battery (b) charge-discharge curve with different bending angles. Charge-discharge curve of battery (c) and (d) at a fixed current of 0.010, 0.020, 0.030, and 0.040 mA (e) and (f) at $1^{st}$, $10^{th}$ and $20^{th}$ cycle. Reproduced with permission from [21] . Copyright (2017) American Chemical Society.

Wang et al. [39] fabricated a linear shaped battery in a one-dimensional structure with omni-directional flexibility. They fabricated a flexible cable-type solid-state rechargeable metal micro-battery of $Zn-MnO_2$ on $MnO_2@CNT$ fiber composite electrode. CNT fiber having a diameter in the range of 80-100 μm is synthesized by direct dry spinning from CNT arrays assembled in floating CVD catalytic reactor. $MnO_2@CNT$ fiber is fabricated by facile electrochemical deposition within aqueous $Mn(NO_3)_2$ solution. This cable type battery is assembled by binder-free MnO2@CNT fiber as cathode and Zn wire as anode, as given as **Figure 19(a)**. From the XRD spectra given in **Figure 19(b)**, it is clear that CNT fiber possesses a graphite like structure with higher crystallinity. XRD pattern of $MnO_2@CNT$ fiber shows that $MnO_2$ grown over CNT surface is as an Arkhtenskite having hexagonal structure with P63/mmc space group. Raman spectra given in **Figure 19(c)** forms a clear difference in D-band, G-band and 2D-band. For the XPS spectra (**Figure 19(d)**) the peaks locate at binding energy 642 eV is assigns to Mn $2p_{3/2}$, confirms that manganese is in chemical state $Mn^{4+}$ as given as **Figure 19(e)**. The CNT fiber in a continuous pattern was synthesized during direct

dry-spinning of CNT formation in the CVD reaction zone, it tends to be wound and going to collected to a mandrel (**Figure 20(a)**). CNT fiber has a diameter in the range of 80-100 μm (**Figure 20(b)**). Also, CNT fiber contains CNT bundles in a diameter range of 10 nm (**Figure 20(c)**). After depositing $MnO_2$ for 30 min, CNT fiber holds a diameter of 100-120 μm (**Figure 20(d)**). From the high-resolution SEM image (**Figure 20(e)** and (**f**)) it is found that $MnO_2$ nanosheets are tends to be intertwined and it going to distribute vertically over the surface of CNT fibers and forming $MnO_2$@CNT composite fiber. EDS spectra shows that element Mn and O is distributing uniformly over the surface of CNT fiber, which confirming deposition of $MnO_2$ on CNT surface given as **Figure 20(g-i)**.
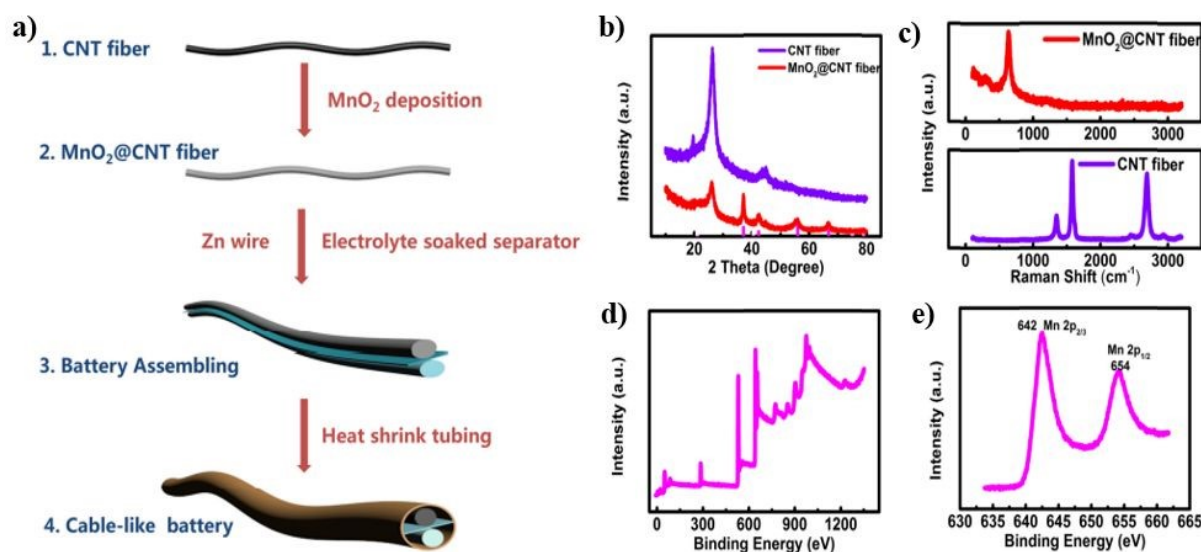


**Figure 19.** (a) Diagrammatic representation of fabrication procedure of Zn-$MnO_2$ cable battery with $MnO_2$@CNT fiber as cathode and Zn wire as anode (b) XRD and (c) Raman Spectra of $MnO_2$@CNT fiber and CNT fiber (d) XPS spectra of $MnO_2$@CNT fiber (e) Mn 2p spectrum of $MnO_2$@CNT composite fiber. Reproduced with permission from[39] . Copyright (2018) American Chemical Society.

Fabricated Zn-$MnO_2$ battery have prominent flexibility, it can able to bend towards any direction without introducing reduction to its performance. **Figure 21(a)** shows that Zn-$MnO_2$ is wrapping around the pen that reveals its efficient electrochemical performance. In order to show the efficiency of battery for the real time application, a LED is connecting which was drive by the two Zn-$MnO_2$ cable batteries as like as **Figure 21(b)**. In order to evaluate its electrochemical capability in different bending states, the cable battery tends to be bending from its normal state (state 1) to a bending state (state 2) as given as **Figure 21(c)** and **(d)**. There is no reduction in electrochemical performance of Zn-$MnO_2$ is clear from **Figure 21(e)**. After completing 100 cycles of consecutive bending, there is not existing any change in charge-discharge curve of cable battery as given as **Figure 21(f)**.
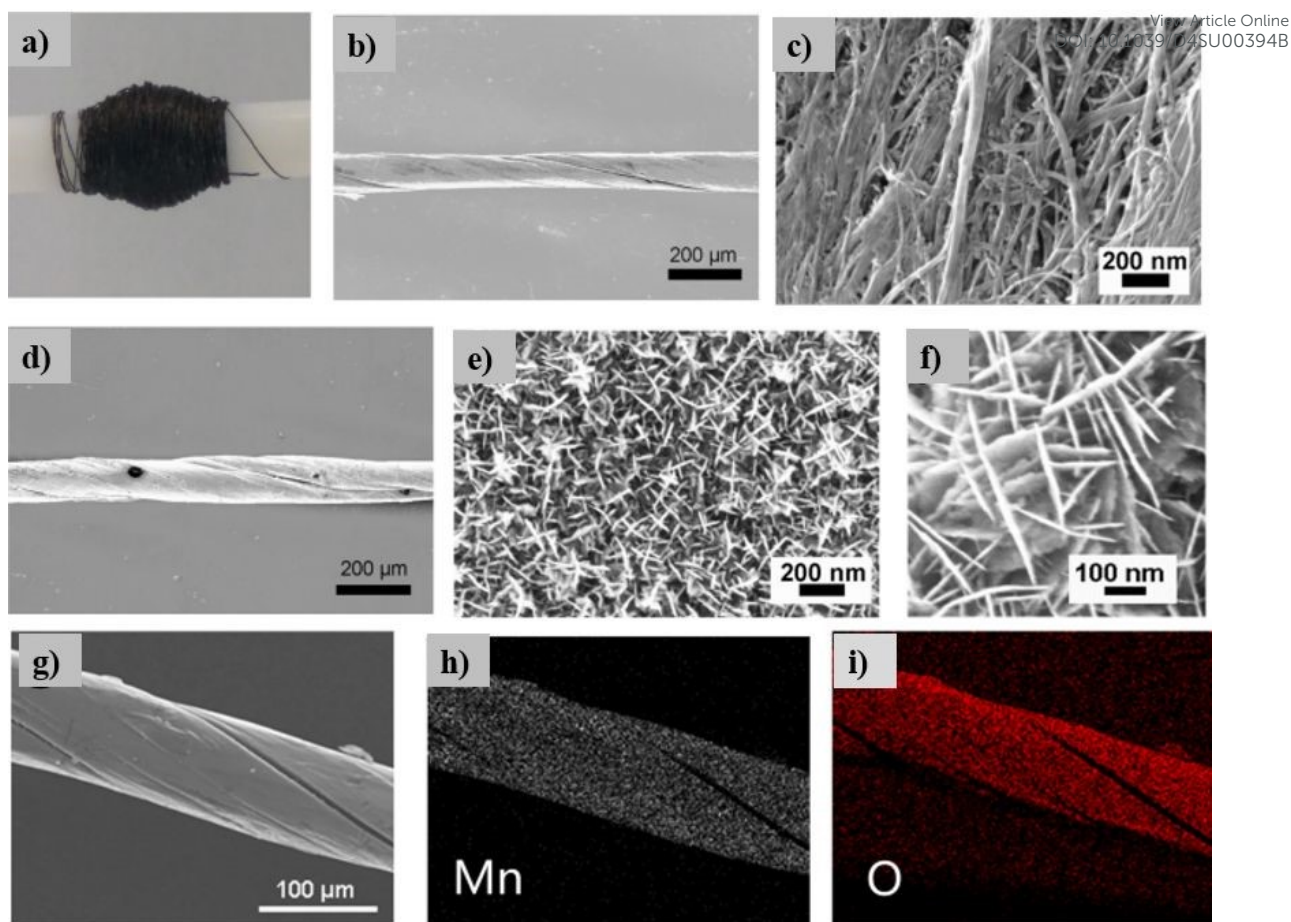
**Figure 20.** (a) Image of CNT fiber twined to a mandrel, (b) and (c) SEM image of CNT fiber in low and higher magnification (d-f) SEM image of $MnO_2$@CNT fiber in various magnifications (g-i) EDS mapping image of $MnO_2$@CNT fiber distributed with Mn and O elements. Reproduced with permission from [39]. Copyright (2018). American Chemical Society.

Developments in the field of flexible energy storage devices introduced an insight into the Ni-Zn batteries. Liu et al.[40] proposed a flexible quasi-solid-state battery prototype with voltage of 1.77V. In the fabricated cell clear from **Figure 22**, ZnO and NiO nanoflakes are going to deposit on the substrate 3D hierarchical carbon cloth- carbon nanofiber (CC-CF) and it act as an anode (CC-CF@ZnO) and cathode (CC-CF@NiO) respectively. CC is going to deposit uniformly coated by 3D N-doped CF arrays which act as a flexible substrate holding large surface area and it act as a suitable basement for oxide loading and this conductive CF is introducing good flexibility and electrical conductivity making an efficient connection with the metal oxides. ZnO nanoparticles are buffering the change in shape and it reducing the growth of Zn dendrite, where a filtered structure is essential for the diffusion of ions. NiO with porous structure and ultrathin layered nature grown on CF is initiating the penetration of electrolyte ions and rapid transportation of ions/mass.
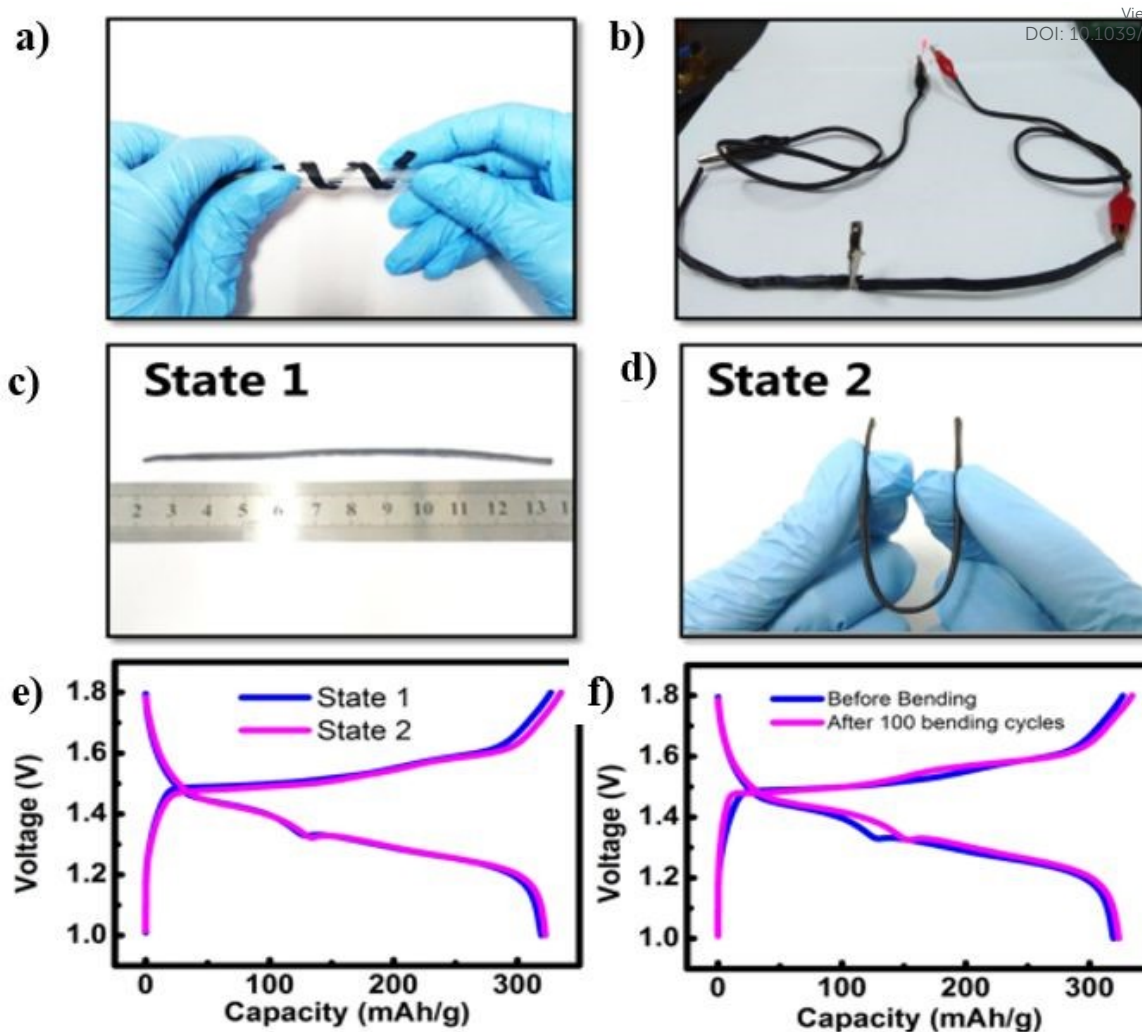
**Figure 21.** (a) Image of Zn-MnO$_2$ cable battery which twin around a roller pen, revealing the twisting (b) Two cable batteries which drive a LED light (c) and (d) Zn-MnO$_2$ cable battery which possess efficient flexibility which bend towards any degree. State 1 is the original state of the battery and state 2 is the bending state (e) GCD curve of Zn-MnO$_2$ before and after 100 cycles. Reproduced with permission from [39]. Copyright (2018) American Chemical Society.

**Figure 22.** Pictorial representation of fabrication procedure of flexible Ni-Zn battery with 3D hierarchical NiO and ZnO coated on CF with N-doped on CC as electrode and its fabrication produced. Reproduced with permission from[40]. Copyright (2016) WILEY-VCH Verlag GmbH & Co. KGaA, Weinheim.

A comparison of CV curve of electrodes CC-CF@ZnO and CC-CF@NiO is analysed at 5 mV/s, where the electrode contains a pair of redox peaks (**Figure 23(a)**). Thereby aqueous fuel cell possessing higher voltage is studied. Thereby, flexible battery was constructed and the CV curve obtained is given in **Figure 23(b).** In the charge-discharge curve taken in various current range of 0.5 to 20 mA/cm$^2$ given as **Figure 23(c)**, it saw that all the curves have a representative charge and discharge plateaus in the range of 1.85 V and 1.75 V, respectively, which consists of hysteresis in voltage at 0.1 V. Even increasing the current density to 20 and 40 times, the fabricated battery still maintains a capacity of 72 and 58.4%, respectively, indicating their efficient rate capability. In order to apply the fabricated electrode material for practical applications, a quasi-solid-state fuel cell device which consists of PVA-KOH gel polymer electrolyte is applied. Charge-discharge curve of fabricated device in a current range of 0.5-10 mA/cm$^2$ is given as **Figure 23(d)**. In addition to the analysis done for aqueous electrolyte, the charge-discharge plateau is comparable with voltage hysteresis with slight increase. This is because of the higher transfer of charge and diffusion resistance of ions with this polymer electrolyte. With increase in the current density, the fabricated device has small value of capacity than the device with aqueous electrolyte (**Figure 23(e)**).
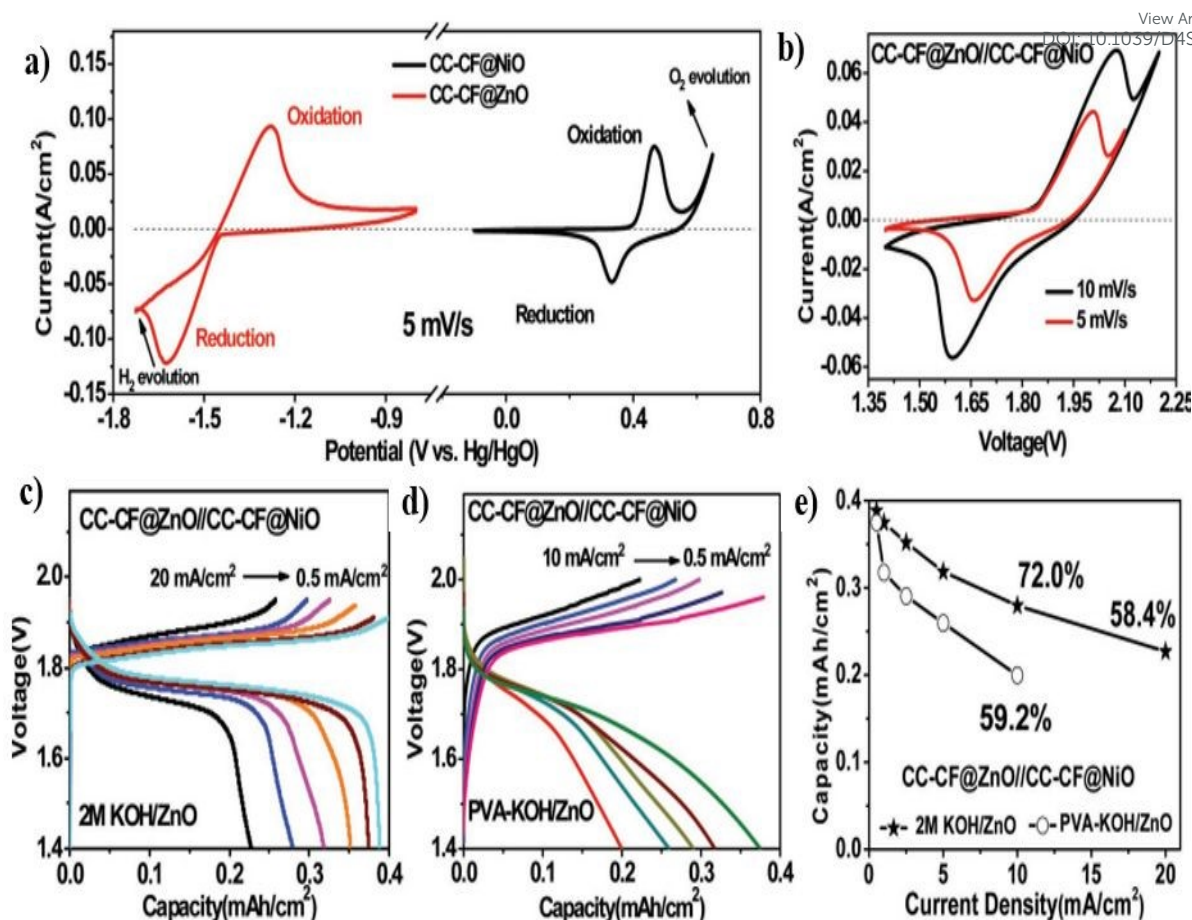
**Figure 23.** (a) CV curve of CC-CF@NiO and CC-CF@ZnO at 5mV/s, (b) CV and (c) charge-discharge curve of aqueous Ni-Zn battery in flexible structure, (d) charge-discharge curve corresponds to flexible Ni-Zn battery, (e) Rate performance of device. Reproduced with permission from[40] Copyright (2016) WILEY-VCH Verlag GmbH & Co. KGaA, Weinheim.

There are large number of reports on CF-based electrode fabrication for the utilization of them in the rechargeable batteries. More details about the reports corresponds to CF-based battery devices are given in **Table 1**.

**Table 1:** Rechargeable battery electrode based on carbon-based fibrous electrodes.

| Electrode | Battery Type | Synthesis Method | Major observation | Ref. |
|---|---|---|---|---|
| **Ni-Metal Organic Framework (MOF)-74 grown on CNTfs** | Ni-Zn battery | Solvothermal method | ⚓ Device assembled to a higher discharge voltage of 1.75 V <br> ⚓ Reversible capacity of 184.5 mAh/cm$^3$ at 0.25 A cm$^{-3}$ <br> ⚓ 186.28 mWh/cm$^3$ and a maximum power density of 8.4 W/cm$^3$ | [41] |

| | | | | |
|---|---|---|---|---|
| **3D CC-ZnO@C-Zn** | Zn-Co battery | In-situ growth followed by deposition of Zn | ■ Higher energy density of 4.6 mWh/cm$^3$ with power density of 0.42 W/cm$^3$ <br> ■ Capacitance retention of 82% after 1600 cycles | [42] |
| **CoO$_x$ encapsulated to carbonized microporous fiber** | ZAB | Electrospinning of ZIF-67 with PAN | ■ Battery holds an initial open circuit voltage of 1.34 V in its flat state and it reaches to 1.33, 1.33 and 1.31 V at a bending angle of 60°, 90° and 120° <br> ■ Galvanostatic cycling at 5 mA/cm$^2$ up to 12 h is found with round-trip efficiency as 49% | [43] |
| **NiFe alloy anchored on N-doped CF derived from bamboo stick** | ZAB | Delignification-impregnation-carbonization strategy | ■ Power density of 102 mW/cm$^2$ and specific capacity of 729 mAh/g <br> ■ The device is cycled for about 150h at 10 mA/cm$^2$ | [44] |
| **Nanocube-like KNiFe(CN)$_6$ (KNHCF) and rugby ball like NaTi$_2$(PO$_4$)$_3$ (NTP) are grown on carbon nanotube fibers as flexible cathode and NTP@CNTF as anode** | Na-ion battery | Chemical bath deposition and chemical etching followed by solvothermal method | ■ Higher capacity of 34.21 mAh/cm$^3$ and energy density of 39.32 mWh/cm$^3$ <br> ■ Prominent mechanical flexibility having only 5.7% capacity retention after bending it for 90º for 3000 cycles | [45] |

## 4. Challenges and Future Perspectives

CFs are considered as a promising future material by assembling it with energy storage devices in order to meet the requirements of flexible and wearable electronic industry. From the present review it is clear that these materials are introducing excellent flexibility and device performance for the host materials that we using for device fabrication. It is possible to synthesize CF-based electrode material in a cost-effective, facile and eco-friendly way thereby we can develop the electronic devices in a feasible method. It is possible to develop a battery-type and capacitive-type material using CF by coating the prescribed material to the fiber substrate by simple drop-casting or spin-coating approaches. From the present study we can found that the analysis on the performance of these fiber-based electrodes is widely done, but the device level applications are less explored.

**RSC Sustainability Accepted Manuscript**
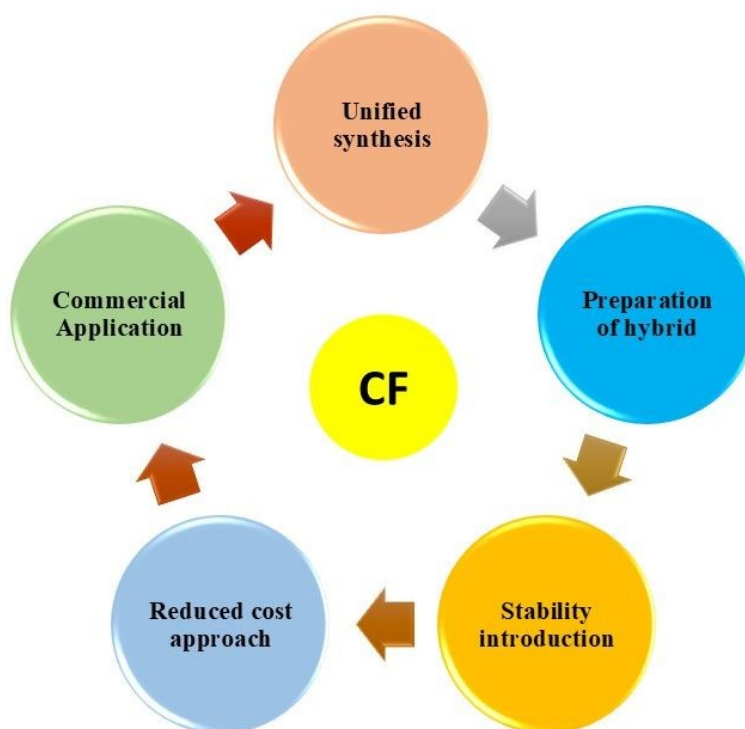


**Figure 24:** Future perspectives of CF-based rechargeable batteries.

The major challenges that stand as a demerit to exploration of CF-based materials in rechargeable batteries are given in **Figure 24** and described below:

- Lack of a unified synthesis approach is a major drawback to exploration of CF-based rechargeable batteries. The rechargeable battery electrode should possess a well-defined architecture with uniform morphology for its demonstration in practical application. Otherwise, it will suffer from deterioration of its performance in terms of morphology alteration after a long-term use.

- The preparation of rechargeable battery electrode materials based on new-generation materials like layered materials, metal organic framework, etc., are lack in the literature. By using these battery-type electrode materials coated on CF substrate will deliver excellent performance characteristics. Less number of reports in this field make destruction in practical device demonstration of CF-based materials.

- Most of the synthesis methods based on CF is through high-cost approaches. But we need a unified synthesis in a reduced cost, especially from biomass-based materials. These biomass materials are highly available in literature and we can extract it in a low-cost manner without using any hard procedure.

- Another demerit underlying with the application of CF-based materials are their reduced stability for a long-term use. There are some stability issues are reported for CF-based ones due to the oxidation, reduction in modulus strength, etc. So, it is very important to incorporate stability by insertion of guest species, optimization of synthesis approach, etc.

It is to be noted here that all these above-mentioned demerits/challenges related to the manufacturing process of CF-based rechargeable batteries affect their possible commercialization. For potential commercialization and the acceptance in the market, low-cost rechargeable batteries should be developed, which necessitates a low-cost and scalable preparation route along with suitable electrode materials. The application of new-generation electrode-active materials such as layered TMDs [46, 47], MXenes [48, 49],

graphitic-carbon nitride [50, 51], etc in the preparation of CF-based electrodes is highly recommended to increase their charge storage potential for commercial batteries whereby CF function either as a substrate material or an additive. A custom-made low-cost CF-based flexible rechargeable batteries may boost the marketability for the wearable electronic gadgetries in the near future.

So, we need a deep level study for the demonstration of these fiber-based electrodes in order to meet the requirements of device demonstrations such as in the field of telecommunication, health-monitoring systems, etc, because the people are always need feasible, flexible and miniaturized-devices to compete their daily life applications. Thus, a further development by the utilization of CF for the practical device applications is necessary, it is sure that we can able to achieve this in the near future.

## 5. Conclusions

We have provided a detailed review on the CF-based fibrous electrodes for flexible battery application. CF is considered as a promising sustainable material for electrochemical energy storage application and it is functioned as a substratum, an electrode-active material or an additive material for application in rechargeable batteries. Different carbon materials such as mesoporous carbons, activated carbons, CNTs, graphene, etc can be combined with CF-based electrodes to achieve high-performance as these can act as large surface area providing electronically conducting templates. CF can be considered as a fantastic sustainable material for developing sustainable rechargeable batteries for a greener future. To meet the demand for the ever-growing flexible and wearable electronic gadgetries, developing flexible and wearable electrochemical energy storage devices is not just a requirement but a necessity. In this review, we discussed the recent developments on the sustainable CF-based fibrous electrodes for application in various rechargeable batteries. The strategies to prepare CF-based flexible electrodes for flexible batteries were discussed with the help of schematic diagrams. The various synthetic approaches such opted for the synthesis such as spray coating, dip-coating, electrochemical deposition etc were explained in detail. The electrochemical performance evaluation of carbon-based fibrous electrodes for batteries was examined using various electrochemical tools such as cyclic voltammetry, galvanostatic charge/discharge measurement, electrochemical impedance spectroscopy, etc. This review proclaims the development of flexible batteries using sustainable CF-based fibrous electrodes.

## Conflicts of Interests

The authors declare no potential conflict of interest.

## Data Availability Statement

Data sharing not applicable – no new data generated. Data availability is not applicable to this article as no new data were created or analysed in this study.

## References

1.      Thomas, S.A. and J. Cherusseri, *A Review of Nb2CT x MXene as an Emerging 2D Material: Synthesis, Applications in Rechargeable Batteries and Supercapacitors, Progress, and Outlook.* Energy & Fuels, 2023.

2.      Farghali, M., et al., *Strategies to save energy in the context of the energy crisis: a review.* Environmental Chemistry Letters, 2023. **21**(4): p. 2003-2039.

3.      Aryee, R., *The Sustainability Onion: A panoramic view of a parent concept, its paths, and progeny.* RSC Sustainability, 2024.

4. Thomas, S.A., J. Cherusseri, and D.N. Rajendran, *Recent Advancements on Carbon Fibers Based Sustainable Electrodes for Flexible and Wearable Supercapacitors.* RSC Sustainability, 2024.

5. Rolandi, A.C., et al., *Unlocking sustainable power: advances in aqueous processing and water-soluble binders for NMC cathodes in high-voltage Li-ion batteries.* RSC Sustainability, 2024.

6. Thomas, S.A. and J. Cherusseri, *Recent Advances in Synthesis and Properties of Zirconium-Based MXenes for Application in Rechargeable Batteries.* Energy Storage: p. e475.

7. Abdah, M.A.A.M., et al., *Facile synthesis of microwave-etched Ti3C2 MXene/activated carbon hybrid for lithium-ion battery anode.* Journal of Electroanalytical Chemistry, 2023. **928**: p. 117050.

8. Kim, T., et al., *Lithium-ion batteries: outlook on present, future, and hybridized technologies.* Journal of materials chemistry A, 2019. **7**(7): p. 2942-2964.

9. Subramaniyam, C.M., et al., *2D layered graphitic carbon nitride sandwiched with reduced graphene oxide as nanoarchitectured anode for highly stable lithium-ion battery.* Electrochimica Acta, 2017. **237**: p. 69-77.

10. Thomas, S.A., J. Cherusseri, and D.N. Rajendran, *Strategically-Designed Hierarchical Polypyrrole-Modified Manganese-Doped Tin Disulfide (SnS2) Nanocomposite Electrodes for Supercapatteries with High Specific Capacity.* Electrochimica Acta, 2024: p. 144910.

11. Yabuuchi, N., et al., *Research development on sodium-ion batteries.* Chemical reviews, 2014. **114**(23): p. 11636-11682.

12. Thomas, S.A., J. Cherusseri, and D.N. Rajendran, *Hierarchical Two-Dimensional Layered Nickel Disulfide (NiS2)@ PEDOT: PSS Nanocomposites as Battery-Type Electrodes for Battery-Type Supercapacitors with High Energy Density.* Electrochem, 2024. **5**(3): p. 298-313.

13. Klaehn, J.R., et al., *Fractional precipitation of Ni and Co double salts from lithium-ion battery leachates.* RSC Sustainability, 2024.

14. Thomas, S.A., J. Cherusseri, and D.N. Rajendran, *Nickel Disulfide (NiS2): A Sustainable Low-Cost Electrode Material for High-Performance Supercapacitors.* Energy Technology, 2024. **12**(7): p. 2400138.

15. Thomas, S.A. and J. Cherusseri, *Boron Carbon Nitride (BCN): Emerging Two-Dimensional Nanomaterial for Supercapacitors.* Journal of Materials Chemistry A, 2023.

16. Ren, Q., Y. Yuan, and S. Wang, *Interfacial strategies for suppression of Mn dissolution in rechargeable battery cathode materials.* ACS Applied Materials & Interfaces, 2021. **14**(20): p. 23022-23032.

17. Thomas, S.A., *Layered two-dimensional black phosphorous-based hybrid electrodes for rechargeable batteries.* Journal of Energy Storage, 2023. **73**: p. 109068.

18. Scandurra, G., A. Arena, and C. Ciofi, *A brief review on flexible electronics for IoT: Solutions for sustainability and new perspectives for designers.* Sensors, 2023. **23**(11): p. 5264.

19. Heng, W., S. Solomon, and W. Gao, *Flexible electronics and devices as human–machine interfaces for medical robotics.* Advanced Materials, 2022. **34**(16): p. 2107902.

20. Majumder, S., T. Mondal, and M.J. Deen, *Wearable sensors for remote health monitoring.* Sensors, 2017. **17**(1): p. 130.

21. De, B., et al., *A facile methodology for the development of a printable and flexible all-solid-state rechargeable battery.* 2017. **9**(23): p. 19870-19880.

22. Ghosh, S., et al., *Multifunctional Utilization of Pitch-Coated Carbon Fibers in Lithium-Based Rechargeable Batteries.* Advanced Energy Materials, 2021. **11**(17): p. 2100135.

23. Cherusseri, J. and K.K. Kar, *Recent progress in nanocomposites based on carbon nanomaterials and electronically conducting polymers.* Polymer nanocomposites based on inorganic and organic nanomaterials, 2015: p. 229-256.

24. Yücel, Y.D., et al., *LiFePO4-coated carbon fibers as positive electrodes in structural batteries: Insights from spray coating technique.* Electrochemistry Communications, 2024. **160**: p. 107670.

25. Marchewka, J., et al., *Characterization of electrochemical deposition of copper and copper (I) oxide on the carbon nanotubes coated stainless steel substrates.* Scientific Reports, 2023. **13**(1): p. 6786.

26. Wang, X., et al., *Controllable preparation of a nano-hydroxyapatite coating on carbon fibers by electrochemical deposition and chemical treatment.* Materials Science and Engineering: C, 2016. **63**: p. 96-105.

27. Tonelli, D., E. Scavetta, and I. Gualandi, *Electrochemical deposition of nanomaterials for electrochemical sensing.* Sensors, 2019. **19**(5): p. 1186.

28. Tang, X. and X. Yan, *Dip-coating for fibrous materials: mechanism, methods and applications.* Journal of Sol-Gel Science and Technology, 2017. **81**: p. 378-404.

29. Petrushenko, D., et al., *Dip-coating of carbon fibers for the development of lithium iron phosphate electrodes for structural lithium-ion batteries.* Energy & Fuels, 2022. **37**(1): p. 711-723.

30. Banea, M.D., L.F. da Silva, and R.D. Campilho, *Principles of adhesive bonding.* Joining of Polymer-Metal Hybrid Structures: Principles and Applications, 2018: p. 3-27.

31. Yin, H., et al., *Tellurium nanotubes grown on carbon fiber cloth as cathode for flexible all-solid-state lithium-tellurium batteries.* 2018. **282**: p. 870-876.

32. Wang, Y., et al., *B, N, F tri-doped lignin-derived carbon nanofibers as an efficient metal-free bifunctional electrocatalyst for ORR and OER in rechargeable liquid/solid-state Zn-air batteries.* 2022. **598**: p. 153891.

33. Liu, C., et al., *Superstructured α-Fe2O3 nanorods as novel binder-free anodes for high-performing fiber-shaped Ni/Fe battery.* 2020. **65**(10): p. 812-819.

34. Qian, Y., et al., *A lightweight 3D Zn@ Cu nanosheets@ activated carbon cloth as long-life anode with large capacity for flexible zinc ion batteries.* 2020. **480**: p. 228871.

35. Ji, D., et al., *Design of 3-dimensional hierarchical architectures of carbon and highly active transition metals (Fe, Co, Ni) as bifunctional oxygen catalysts for hybrid lithium–air batteries.* 2017. **29**(4): p. 1665-1675.

36. Hou, Z., et al., *Nanostructured Co3O4 Asymmetrically Deposited on a Single Carbon Cloth for an All-Solid-State Integrated Hybrid Device with Reversible Zinc-Air High-Energy Conversion and Asymmetric Supercapacitive High-Power Delivery.* 2021. **35**(15): p. 12706-12717.

37. Pendashteh, A., et al., *Doping of self-standing cnt fibers: promising flexible air-cathodes for high-energy-density structural zn–air batteries.* 2018. **1**(6): p. 2434-2439.

38. Du, T., et al., *A universal strategy to fabricate metal sulfides@ carbon fibers as freestanding and flexible anodes for high-performance lithium/sodium storage.* 2019. **2**(6): p. 4421-4427.

39. Wang, K., et al., *High-performance cable-type flexible rechargeable Zn battery based on MnO2@ CNT fiber microelectrode.* 2018. **10**(29): p. 24573-24582.

40. Liu, J., et al., *A flexible quasi-solid-state nickel–zinc battery with high energy and power densities based on 3D electrode design.* 2016. **28**(39): p. 8732-8739.

41. Man, P., et al., *A one-dimensional channel self-standing MOF cathode for ultrahigh-energy-density flexible Ni–Zn batteries.* 2019. **7**(48): p. 27217-27224.

42. Li, M., et al., *Finely Crafted 3D Electrodes for Dendrite-Free and High-Performance Flexible Fiber-Shaped Zn–Co Batteries.* 2018. **28**(32): p. 1802016.

43. Yang, C., et al., *Nitrogen-doped carbon fibers embedding CoO x nanoframes towards wearable energy storage.* 2020. **12**(16): p. 8922-8933.

44. Niu, Y., et al., *A bimetallic alloy anchored on biomass-derived porous N-doped carbon fibers as a self-supporting bifunctional oxygen electrocatalyst for flexible Zn–air batteries.* 2020. **8**(27): p. 13725-13734.

RSC Sustainability Accepted Manuscript

45.    He, B., et al., *All binder-free electrodes for high-performance wearable aqueous rechargeable sodium-ion batteries.* 2019. **11**(1): p. 1-12.

46.    Thomas, S.A., J. Cherusseri, and D. N. Rajendran, *2D Nickel Sulfide Electrodes with Superior Electrochemical Thermal Stability along with Long Cyclic Stability for Supercapatteries.* Energy Technology, 2024: p. 2301641.

47.    Singh, E., et al., *Flexible molybdenum disulfide (MoS2) atomic layers for wearable electronics and optoelectronics.* ACS applied materials & interfaces, 2019. **11**(12): p. 11061-11105.

48.    Zaed, M., et al., *Low-cost synthesis of Ti3C2Tx MXene-based sponge for solar steam generation and clean water production.* Ceramics International, 2024.

49.    Asad, S., et al., *Recent Advances in Titanium Carbide MXene (Ti3C2T x) Cathode Material for Lithium–Air Battery.* ACS Applied Energy Materials, 2022. **5**(10): p. 11933-11946.

50.    Thomas, S.A., et al., *Graphitic Carbon Nitride and Their Derivatives*, in *Handbook of Functionalized Carbon Nanostructures: From Synthesis Methods to Applications*. 2024, Springer. p. 1-38.

51.    Inagaki, M., et al., *Graphitic carbon nitrides (g-C3N4) with comparative discussion to carbon materials.* Carbon, 2019. **141**: p. 580-607.

**RSC Sustainability Accepted Manuscript**

## Data Availability Statement

Data sharing not applicable – no new data generated. Data availability is not applicable to this article as no new data were created or analysed in this study.